U.S. DEPARTMENT OF COMMERCE
Environmental Science Services Administration
Research Laboratories

ESSA Technical Memorandum ERLTM-NSSL 45

ON THE RELATIONSHIP BETWEEN HORIZONTAL MOISTURE CONVERGENCE AND CONVECTIVE CLOUD FORMATION

Horace R. Hudson

National Severe Storms Laboratory
Norman, Oklahoma
March 1970

FOREWORD

The work reported here has been jointly supported by the National Severe Storms Laboratory, ESSA Research Laboratories, and the Techniques Development Laboratory, ESSA Weather Bureau. It has involved facilities at the National Severe Storms Laboratory, Norman, Oklahoma, and at the National Severe Storms Forecast Center, Kansas City, Missouri, and personnel of these organizations working together to develop improved techniques for severe storm forecasting.

TABLE OF CONTENTS

FOREWORD	ii
FIGURES	v
LIST OF MATHEMATICAL SYMBOLS	vii
LIST OF SYMBOLS FOR RADAR SUMMARY CHARTS	viii
ABSTRACT	x
1. INTRODUCTION	1
2. THEORY	1
3. DATA	4
4. COMPUTATIONS	5
5. PROCEDURES	6
6. RELATION OF Q_1 TO STABILITY INDICES	8
7. EXAMPLES	8
7.1 Case 1 - 14 May 1967	9
7.2 Case 2 - 3 April 1968	10
7.3 Case 3 - 15 May 1968	16
8. CONCLUSIONS	22
9. ACKNOWLEDGEMENTS	28
10. REFERENCES	28

FIGURES

Figure		Page
1	The area of analysis and the grid. United States rawinsonde stations are shown by black dots.	6
2	Relationship between Q_1, the temperature portion of the moisture requirement, and the Lifted Index.	8
3A	Surface analysis for 0600 CST, 14 May 1967. Lines are isobars.	11
3B	500-mb analysis for 0600 CST, 14 May 1967. Height contours are indicated by solid lines and are in tens of feet. Isotherms are indicated by dashed lines and are in °C.	11
3C	Surface analysis for 1800 CST, 14 May 1967. Lines are isobars.	11
3D	500-mb analysis for 1800 CST, 14 May 1967. Height contours are indicated by solid lines and are in tens of feet. Isotherms are indicated by dashed lines and are in °C.	11
4A	Horizontal moisture divergence field (positive values indicate convergence) in the layer from the surface to 10,000 ft MSL for 0600 CST, 14 May 1967. Units are grams cm^{-2} $hour^{-1}$ in the column times 100.	12
4B	Moisture requirement field in the layer from the lifting condensation level to 400 mb. Units are grams cm^{-2} in the column.	12
4C	Lifted height field for 0600 CST, 14 May 1967. Contours are in hundreds of feet. The 7000-ft contour is dashed.	12
4D	Percent coverage field in percent for 0600 CST, 14 May 1967.	12
4E	Radar echo patterns at 0545 CST, 14 May 1967.	13
4F	Radar echo patterns at 0845 CST, 14 May 1967.	13
4G	Radar echo patterns at 1145 CST, 14 May 1967.	13
5A	Horizontal moisture divergence field for 1800 CST, 14 May 1967.	14
5B	Moisture requirement field for 1800 CST, 14 May 1967.	14
5C	Lifted height field for 1800 CST, 14 May 1967.	14
5D	Percent coverage field for 1800 CST, 14 May 1967.	14
5E	Radar echo patterns at 1745 CST, 14 May 1967.	15
5F	Radar echo patterns at 2045 CST, 14 May 1967.	15
5G	Radar echo patterns at 2345 CST, 14 May 1967.	15

6A Surface analysis for 0600 CST, 3 April 1968. 17
6B 500-mb analysis for 0600 CST, 3 April 1968. 17
6C Surface analysis for 1800 CST, 3 April 1968. 17
6D 500-mb analysis for 1800 CST, 3 April 1968. 17
7A Horizontal moisture divergence field for 0600 CST, 3 April 1968. 18
7B Moisture requirement field for 0600 CST, 3 April 1968. 18
7C Lifted height field for 0600 CST, 3 April 1968. 18
7D Percent coverage field for 0600 CST, 3 April 1968. 18
7E Radar echo patterns at 0545 CST, 3 April 1968. 19
7F Radar echo patterns at 0845 CST, 3 April 1968. 19
7G Radar echo patterns at 1145 CST, 3 April 1968. 19
8A Horizontal moisture divergence field for 1800 CST, 3 April 1968. 20
8B Moisture requirement field for 1800 CST, 3 April 1968. 20
8C Lifted height field for 1800 CST, 3 April 1968. 20
8D Percent coverage field for 1800 CST, 3 April 1968. 20
8E Radar echo patterns at 1745 CST, 3 April 1968. 21
8F Radar echo patterns at 2045 CST, 3 April 1968. 21
8G Radar echo patterns at 2345 CST, 3 April 1968. 21
9A Surface analysis for 0600 CST, 15 May 1968. 23
9B 500-mb analysis for 0600 CST, 15 May 1968. 23
9C Surface analysis for 1800 CST, 15 May 1968. 23
9D 500-mb analysis for 1800 CST, 15 May 1968. 23
10A Horizontal moisture divergence for 0600 CST, 15 May 1968. 24
10B Moisture requirement field for 0600 CST, 15 May 1968. 24
10C Lifted height field for 0600 CST, 15 May 1968. 24
10D Percent coverage field for 0600 CST, 15 May 1968. 24
10E Radar echo patterns at 0545 CST, 15 May 1968. 25
10F Radar echo patterns at 0845 CST, 15 May 1968. 25
10G Radar echo patterns at 1145 CST, 15 May 1968. 25
11A Horizontal moisture divergence field for 1800 CST, 15 May 1968. 26
11B Moisture requirement field for 1800 CST, 15 May 1968. 26

11C Lifted height field for 1800 CST, 15 May 1968. 26
11D Percent coverage field for 1800 CST, 15 May 1968. 26
11E Radar echo patterns at 1745 CST, 15 May 1968. 27
11F Radar echo patterns at 2045 CST, 15 May 1968. 27
11G Radar echo patterns at 2345 CST, 15 May 1968. 27

LIST OF MATHEMATICAL SYMBOLS

a	mean radius of the earth
c_p	specific heat capacity at constant pressure
c_v	specific heat capacity at constant volume
D	dew-point depression
g	acceleration of gravity
h	heat per unit mass
L	latent heat of condensation
LCL	lifting condensation level
LI	lifted index
P	pressure
Q	total moisture requirement
Q_1	temperature component of Q
Q_2	moisture component of Q
q	mixing ratio
q_s	saturation mixing ratio
R	gas constant for dry air
T	temperature (Kelvin)
T^*	virtual temperature (Kelvin)
t_{LCL}	temperature at LCL (Celsius)
T_s	saturation temperature (Kelvin)
t	temperature (Celsius); time
t_d	dew-point temperature (Celsius)
U	zonal component (along X-axis) of $\mathbb{V}$
u	component of $\mathbb{V}$ along the x-axis
$\mathbb{V}$	horizontal wind velocity
V	meridional component (along Y-axis) of $\mathbb{V}$

v	component of $\mathbb{V}$ along the y-axis
X	curvilinear distance along latitude circle
x	axis of a rectangular grid along a standard longitude on the image plane of a polar stereographic map projection
Y	curvilinear distance along a longitude circle
y	axis of a rectangular grid perpendicular to a standard longitude on the image plane of a polar stereographic map projection
z	height
α	specific volume = $1/\rho$
ϕ	latitude
ϕ_o	standard latitude (60°N)
ρ	density of air
σ	image scale factor
θ_w	wet bulb potential temperature

LIST OF SYMBOLS FOR RADAR SUMMARY CHARTS

⊙	less than 0.1 coverage	amount of radar echo
◐	0.1 to 0.5 coverage	
◑	0.6 to 0.9 coverage	
⊕	over 0.9 coverage	
R	rain	type of surface weather associated with echo
RW	rain showers	
S	snow	
SW	snow showers	
T	thunderstorm	
--	very light	intensity of precipitation
-	light	
no sign	moderate	
+	heavy	
++	very heavy	
U	unknown	

-+	decreasing rapidly	intensity tendency
--	decreasing slowly	
-	decreasing	
NC	no change	
+	increasing	
+-	increasing slowly	
++	increasing rapidly	
hhh	height of echo tops	height in hundreds of feet MSL
hhh	maximum height of echo tops	

LN preceding the weather type indicates a line of echoes; otherwise the symbols refer to an area of echoes.

The intensity tendency symbol follows intensity of the echo symbol and is preceded by a slash.

Example: LN TRW + / -- means that a line of thunderstorms and heavy rain showers are occuring and are decreasing slowly in intensity.

ABSTRACT

A technique suggested by H. L. Kuo for parameterizing the net effect of the latent heat released by cumulus convection on large scale flow is evaluated to determine its applicability to regions of convection in middle latitude severe storm situations. The ratio of the integrated horizontal moisture divergence to a measure of moisture required for the development of a model cloud is interpreted as the amount of model cloud produced in a given time. The model cloud is characterized by pseudo-adiabatic temperature and moisture profiles above the lifting condensation level. The technique uses regularly available rawinsonde data and is performed using computer techniques.

Results suggest that well-defined axes of horizontal moisture convergence generally accompany development of strong cumulus convection and that the use of a pseudo-adiabatic cloud to model the moisture requirements generally gives a reasonable amount of predicted cloud formation. The patterns of predicted cloud formation often correlate well with observed radar patterns of strong cumulus convection. Generally, the correlation, which is based on radar data at three hour intervals, is good at rawinsonde observation time, a little better three hours later, and decreases at greater time intervals between rawinsonde and radar observation time. Thus, this parameterization technique can be used as a kinematic short-range forecasting aid and possibly in numerical models designed for prediction of cumulus convection.

ON THE RELATIONSHIP BETWEEN HORIZONTAL MOISTURE CONVERGENCE AND CONVECTIVE CLOUD FORMATION

Horace R. Hudson

1. INTRODUCTION

Several investigators (e.g., Ooyama, 1963, Charney and Eliassen 1964, Kuo, 1964, and Sasaki, 1964) have attempted to devise methods to include, in the governing equations of large scale flow, the effect of the latent heat released by cumulus convection in a conditionally unstable atmosphere. A theoretical parameterization of the convective scale motions is required to include their net effect without the use of a model capable of describing such motions in detail. This study applies Kuo's technique to middle latitude severe storm situations and evaluates its use in determining regions of convective activity in these cases. Krishnamurti (1968) similarly applied Kuo's theory to the study of an easterly wave positioned below a cold low in the tropics.

The amount of moisture per unit area required to produce a model cloud whose temperature and moisture profiles are pseudo-adiabatic in a layer representative of moderate cumulus convection is calculated. The base of the layer is the lifting condensation level (LCL)[1], the level of saturation of moist air raised with dry adiabatic expansion, and the top is 400 mb (approximately 24,000 feet). The amount of model cloud produced by the horizontal moisture convergence in the layer bounded by the surface of the earth and sufficiently thick to contain most of the atmospheric water vapor is determined. The top of the layer was chosen to be 10,000 feet above sea level. The amount of model cloud produced is compared with the convective activity indicated by the U.S. Weather Bureau radar network and by severe weather reports.

2. THEORY

According to Kuo (1965) the moisture that must be added to a vertical column of air of unit horizontal area possessing a given temperature and moisture profile to produce the model cloud can be considered to be composed of two parts:

a) Q_1, the amount required to warm the column from the environmental temperature to that of the appropriate pseudo-adiabat by the

[1] A List of Symbols appears at the front of this paper.

release of latent heat, and

b) Q_2, the amount required to saturate the column at the pseudo-adiabatic temperature.

The first part can be obtained from the First Law of Thermodynamics by equating the latent heat of the vapor condensed dh, to the change in the internal plus potential energy:

$$dh = d(Lq) = c_v dT + Pd\alpha = c_p dT - \alpha dP, \tag{1}$$

where L is the latent heat of condensation and is considered a constant, q the mixing ratio, c_v the specific heat at constant volume, T the temperature, P the pressure, α the specific heat at constant pressure.

Consider a constant pressure process in which the amount of water vapor that must be condensed per gram of dry air in order to raise the temperature from T, the environmental temperature, to T_s, the saturation temperature at the same level, is:

$$dq = \frac{c_p}{L} \int_T^{T_s} dT = \frac{c_p}{L} (T_s - T). \tag{2}$$

The amount of water vapor required to produce the temperature change in a column dZ high is:

$$\rho dq dZ = -\frac{1}{g} dq dP = -\frac{c_p}{gL} (T_s - T) dP, \tag{3}$$

where ρ is the density of air and g is the acceleration of gravity.

Integrating through the column with respect to pressure, we obtain:

$$Q_1 = -\frac{c_p}{gL} \int_{P_B}^{P_T} (T_s - T) dP, \tag{4}$$

where Q_1 has units of grams of water vapor per unit area through the column, P_B is the pressure at the bottom of the column, and P_T is the pressure at the top.

The water vapor needed to saturate the column is:

$$Q_2 = -\frac{1}{g} \int_{P_B}^{P_T} (q_s - q) dP, \tag{5}$$

where q_s is the saturation mixing ratio of the pseudo-adiabat of the model cloud.

The total moisture requirement is:

$$Q = Q_1 + Q_2. \tag{6}$$

The horizontal moisture divergence in spherical coordinates is:

$$\nabla_H \cdot (\rho q \mathbf{V}) = \frac{\partial(\rho q U)}{\partial X} + \frac{\partial(\rho q V)}{\partial Y} - \frac{\rho q V \tan\phi}{a}, \tag{7}$$

where $\mathbf{V}$ is the horizontal wind velocity, U and V are zonal and meridional components of $\mathbf{V}$, respectively, X and Y are curvilinear distances along latitude and longitude circles, respectively, a is the mean radius of the earth, and ϕ is the latitude.

Using Phillips' (1957) expression for divergence on the polar stereographic map projection, (7) becomes:

$$\nabla_H \cdot (\rho q \mathbf{V}) = \sigma^2 \left[\frac{\partial(\rho q u/\sigma)}{\partial x} + \frac{\partial(\rho q v/\sigma)}{\partial y}\right]. \tag{8}$$

In (8), σ is the image scale factor,

$$\sigma = \frac{1 + \sin \phi_o}{1 + \sin \phi},$$

ϕ_o is the standard latitude 60°N, and u and v are the components of $\mathbf{V}$ along the x- and y-axes of a rectangular grid on the image plane.

The integrated horizontal moisture divergence in a column bounded below by the surface of the earth at Z_o and above by a level Z_1 at a constant height above sea level is:

$$\int_{Z_o}^{Z_1} \nabla_H \cdot (\rho q \mathbf{V}) dZ = \nabla_H \cdot \int_{Z_o}^{Z_1} \rho q \mathbf{V} dz - \nabla_H Z_1 \cdot (\rho q \mathbf{V})_{Z_1} + \nabla_H Z_o \cdot (\rho q \mathbf{V})_{Z_o}. \tag{9}$$

The second term on the right in (9) is zero because $\nabla_H Z_1 = 0$. The surface terrain is generally level over most of the region covered by the grid; consequently, the third term on the right is generally small and is neglected in this study.

Substitution for ρ in (8) from the equation of state for moist air and then substitution into (9) yields:

$$\int_{Z_o}^{Z_1} \nabla_H \cdot (\rho q \mathbf{V}) dZ = \sigma^2 \frac{\partial}{\partial x} \int_{Z_o}^{Z_1} \frac{pqu}{RT^*\sigma} dZ + \sigma^2 \frac{\partial}{\partial y} \int_{Z_o}^{Z_1} \frac{pqv}{RT^*\sigma} dZ, \qquad (10)$$

where R is the gas constant for dry air and T* is the virtual temperature.

The horizontal moisture divergence that appears on the left side of (10) can be expanded to show two factors commonly used in forecasting cumulus convection--divergence of the velocity field and moisture advection by the velocity field:

$$\nabla_H \cdot (\rho q \mathbf{V}) = \rho q \nabla_H \cdot \mathbf{V} + \mathbf{V} \cdot \nabla_H (\rho q). \qquad (11)$$

Vertical motion fields calculated at 10,000 ft from the horizontal velocity divergence in the layer from the surface to 10,000 ft are very similar to patterns of horizontal moisture divergence in this layer. The two terms on the right in (11) generally have the same sign where cyclone scale development occurs, but the pattern of their sum, the horizontal moisture divergence, closely resembles that of the vertical motion field.

The horizontal moisture convergence, multiplied by the number of hours Δt over which it occurs and divided by the moisture requirement, can be interpreted as the fraction of convective cloud cover produced in the column during time Δt. For the processes being considered here Δt is of the order of a few hours. Calculations are made for a unit time interval of 1 hour for ease in considering time increments in multiples of 1 hour.

3. DATA

Nine periods with severe weather occurrences were chosen for study as shown in table 1. These periods range in length from one day to four days (two to eight rawinsonde observation times) and are represented in 30 times of observation. The National Meteorological Center provided the 1967 data, and the National Severe Storms Forecast Center (NSSFC) provided the 1968 data. The radiosonde data were checked for consistency using the operational checking program at NSSFC (Inman, 1968).

Table 1. Rawinsonde Data

First observation time in case	Number of consecutive observation times in case
0600 CST 14 May 1967	2
0600 CST 30 May 1967	2
0600 CST 9 June 1967	4
0600 CST 3 April 1968	4
0600 CST 14 April 1968	2
0600 CST 16 April 1968	2
0600 CST 6 May 1968	4
0600 CST 14 May 1968	8
0600 CST 10 June 1968	2

4. COMPUTATIONS

The pseudo-adiabat that defines the model cloud is characterized by the wet bulb potential temperature $\overline{\theta}_w$ of a parcel of air whose thermodynamic properties are representative of the lowest 100-mb surface layer. The average temperature and mixing ratio of this layer for evening soundings (1800 CST) were used as parcel properties, but allowance for daytime surface heating was made in the morning soundings (0600 CST) by adding 2°C to the observed temperature 100 mb above the surface and then assuming a dry adiabatic lapse rate from that point to the surface.

The wet bulb potential temperature $\overline{\theta}_w$ was calculated using an empirical relation reported by Prosser and Foster (1966)[2]. Temperatures at reported pressure levels were calculated for the pseudo-adiabats $\overline{\theta}_w$ = 10°C, 20°C, and 30°C using a third-order polynomial for each pseudo-adiabat. The temperatures along the pseudo-adiabat $\overline{\theta}_w$ were interpolated using the temperature of the nearest two of the three pseudo-adiabats.

A check was made for "overrunning," a condition consisting of a layer of relatively cool, dry air at the surface and relatively warm, moist air above. If the lift occurs mostly in the warm air, calculations based on conditions in the lower layer do not represent the dominant physical processes.

This situation was identified by computing wet bulb temperatures at each reported pressure level between the top of the surface layer

[2] Calculations discussed in the first four paragraphs of this section are described by Prosser and Foster (1966).

and 700 mb and comparing them with the temperatures of the parcel lifted along the pseudo-adiabat through $\overline{\theta}_w$. If the wet bulb temperature exceeded the parcel temperature, the level at which this difference was the largest was taken to be the new starting level of the parcel.

The temperature at the LCL was determined using the following equation (Inman, 1969).

$$t_{LCL} = t_d - D(0.212 - 0.001571t_d - 0.000436t), \qquad (12)$$

where t and t_d are the temperature and dew point in degrees Celsius respectively, and D is the dew point depression. The pressure at the LCL was obtained from Poisson's adiabatic equation for a perfect gas.

The total moisture requirement, the distance that the parcel must be lifted to attain saturation (lifted height), and the two integrals in the horizontal moisture divergence of (10) were obtained for each rawinsonde report and then, with an objective analysis scheme, at grid points at a spacing of 68.5 nautical miles for the eastern two-thirds of the United States (fig. 1). Finally, the field of integrated horizontal moisture divergence was determined.

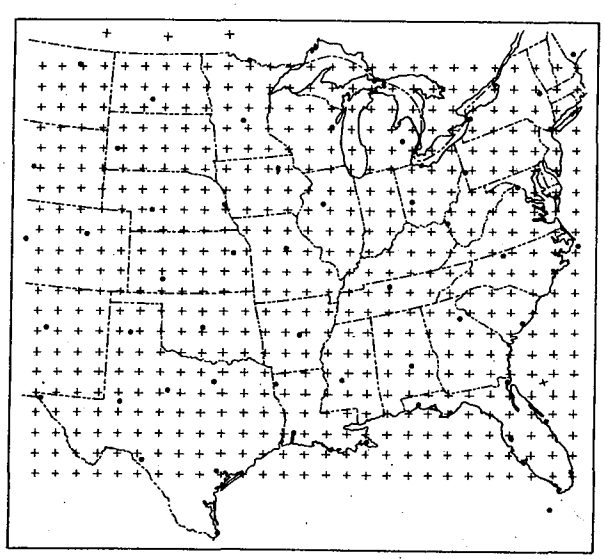

Figure 1. The area of analysis and the grid. United States rawinsonde stations are shown by black dots.

The scheme of the objective analysis (Inman, 1970) is a successive approximation procedure similar to that developed by Cressman (1959), but modified in a manner devised by Endlich and Mancuso (1968) so that observations along the wind direction contribute more than do crosswind observations to a grid point value.

5. PROCEDURES

Station values of the moisture requirement are calculated for the layer from the LCL to 400 mb rather than to the level near the tropopause at which the parcel becomes colder than the environment, the top of the cloud according to parcel theory. This level is generally above 400 mb when moderate or strong convection is likely to occur. Computations were not made to a higher level, because

above 400 mb the loss of thermodynamic sounding data becomes significant, there is little moisture, and the environment-parcel temperature difference is generally small. Thus, the moisture requirement is a little low when the temperature of the parcel is warmer than that of the environment at 400 mb. When the parcel is colder than the environment at 400 mb, it may be colder than the environment in the entire layer from the LCL to 400 mb. In this case, Q_1 is almost always larger in magnitude than Q_2. Thus, the total moisture requirement is negative, which for the purposes of this study is all that is required.

Since most of the water vapor is below 10,000 ft (MSL) and loss of wind data becomes significant above 10,000 ft (MSL), it was decided that the layer of integration of the horizontal moisture divergence should not extend higher than 10,000 ft (MSL). The divergence was calculated for two layers for several test cases: surface to 6000 ft (MSL) and surface to 10,000 ft (MSL). Patterns of divergence were similar for the two layers, and the values were larger for the second layer than for the first. Since the results were so similar, it was decided to use the layer up to 10,000 ft (MSL), as it is thicker and thus probably more representative of the horizontal moisture divergence.

The percent coverage, the ratio of the integrated horizontal moisture divergence multiplied by 1 hour to the moisture requirement, expressed in percent was calculated only at grid points where moisture convergence was occurring and where the moisture requirement was positive, since cumulus convection can occur in this model only under these conditions.

The percent coverage occasionally exceeded 100 percent and may then, perhaps, be considered in terms of production of cloud air. This condition often occurred when the horizontal moisture convergence and the moisture requirement were both small; one example of this is presented by soundings in the southwestern United States. There the atmosphere is generally quite dry, and the LCL is high. This reduces the layer of integration and the moisture requirement. At the same time the horizontal moisture convergence is small because the low level air is dry. The calculated percent coverage under these conditions can become unrealistically large even though appreciable cumulus convection is unlikely. Thus, grid point percentages are set to zero when the parcel must be lifted more than 7,000 ft (a little more than 200 mb in the lower layers), and the moisture requirement is less than 0.7 grams per cm^2, values chosen by a qualitative examination of several test cases. These criteria are not very restrictive, as shown in the cases discussed in section 7. It is a physically realistic modification, however.

When the percent coverage exceeds 100 percent and the above criteria are not met, the percent coverage is set equal to 100 percent.

6. RELATION OF Q_1 TO STABILITY INDICES

The calculation of Q_1, the amount of water vapor associated with the required temperature change in the column, consists of determining the area on a thermodynamic diagram between the environmental temperature profile and the pseudo-adiabat of the cloud profile in the layer from the LCL to 400 mb. This area is proportional to the kinetic energy change of a parcel rising along that pseudoadiabat and is a representation of the stability of the sounding. Stability indices such as the Showalter Index (Showalter, 1953) and the Lifted Index (Galway, 1956) are commonly used estimates of this energy change in somewhat different layers. Since the Lifted Index (LI) is calculated in determining Q_1, the relationship between Q_1 and LI was examined to show how Q_1 is related to a commonly used stability parameter.

The Lifted Index is the difference between the observed 500-mb temperature and the 500-mb temperature of a mean parcel lifted adiabatically from a modified lowest 3,000-ft-thick surface layer. The lowest 100-mb layer is used in this study instead, and overrunning cases with LI based on data at a single level aloft are included.

The association between Q_1 and LI is indicated in figure 2 by plots of 525 observations, approximately half morning and half evening soundings. The relationship is nearly linear, verifying that the lifted index is a good estimate of the stability of the atmosphere as represented by the parcel process.

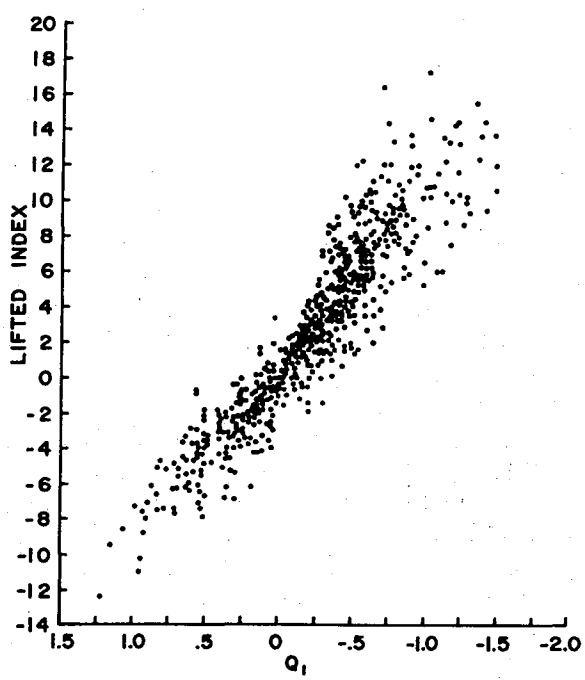

Figure 2. Relationship between Q_1, the temperature portion of the moisture requirement, and the Lifted Index.

7. EXAMPLES

It is virtually impossible to obtain detailed quantitative information on the distribution of strong cumulus convection over the region of the grid; thus, the computed results can be evaluated only qualitatively.

The 32 data sets available for the 8 periods shown in table 1 were computer-processed, and the fields of horizontal moisture divergence, moisture requirements, and predicted percent coverage were compared with radar echo patterns and with severe weather reports. U. S. Weather Bureau radar summary charts, available at 3-hour intervals for the times and areas of interest, provided radar echo

patterns. Severe weather reports were obtained from Storm Data (1967, 1968).

Morning and evening data for three days were chosen as typical and are discussed in detail in the final section. Synoptic patterns and severe weather occurrences for the two 1968 cases are discussed briefly by Pearson (1968).

7.1 Case 1 - 14 May 1967

At 0600 CST on 14 May 1967 a surface frontal system extended from South Carolina to Kentucky and into central Texas (fig. 3A). The surface low in western Arkansas became dominant and moved to eastern Arkansas between 0600 and 1800 CST (fig. 3C). The southern portion of a large 500-mb trough that extended southwestward from a low centered near Hudson Bay moved from western New Mexico to the Texas panhandle during the day (figs. 3B and 3D).

An axis of horizontal moisture convergence[3] (fig. 4A) lay from eastern Texas through Oklahoma to northern Kentucky. Areas of large moisture divergence were centered in northern Texas and Mississippi. A minimum in the lifted height field (fig. 4C) occurred in western Oklahoma where low-level velocity divergence and dry advection occurred. Moisture requirements (fig. 4B) are high over most of the southeastern United States with an axis of maximum values extending from southern Texas to Tennessee. The minima in the lifted height field in western Illinois occurred near the region of maximum horizontal moisture convergence and probably defined the area of maximum low-level moisture.

Radar echo patterns were better organized at 0845 CST (fig. 4F) and 1145 CST (fig. 4G) than at 0545 CST (fig. 4E). The radar echo patterns at 0845 CST agreed well with the percent coverage field (fig. 4D). By 1145 CST the thunderstorm activity had begun to move southeastward from the percent coverage field pattern.

At 0545 CST rain and thundershowers over the lower Mississippi Valley occurred in an area of zero percent coverage. By 0845 CST this area had dissipated, suggesting the predictive nature of the model.

The small areas of rain and thundershowers north of the primary convective area weakened during the morning and occurred in an area of zero percent coverage.

---

[3] Contrary to convention, positive values indicate convergence and negative values divergence in figures 4A, 5A, 7A, 8A, 10A, and 11A.

Hail was reported in south central Oklahoma at about 0600 CST just outside of the nonzero percent area. Heavy rains and three funnels occurred in Kentucky during the morning.

By 1800 CST the axis of horizontal moisture convergence (fig. 5A) extended from the Louisiana coast to western Tennessee. The area of divergence behind the front was still present. The axis of minimum lifted height (fig. 5C) agreed quite well with the radar echo pattern at 1800 CST. Moisture requirements (fig. 5B) decreased over most of the region that had positive values at 0600 CST.

At 1800 CST the cloud cover percentage patterns (fig. 5D) were not quite as accurate as those 12 hours earlier, but most of the principal feature - the squall line extending from Kentucky southwestward to the Gulf Coast - was within the nonzero area. However, the area of thundershowers over Indiana and northern Kentucky at 1800 did not show up because of the moisture divergence in the region. No convection was predicted over most of the area of light rain north of the front (fig. 5E-G). Light rain and some thundershowers were occurring in the northeastern United States where the percentages were very large. Generally, these large percentages resulted from small values of convergence and moisture requirements.

Severe weather reports between 1800 and 2400 CST included a hailstorm near Shreveport, Louisiana (SHV), and funnels, strong winds, and heavy rains in east central Alabama and northern Georgia. All of these occurrences were within nonzero areas.

7.2 Case 2 - 3 April 1968

The center of a large, well-organized surface low moved from southwestern Nebraska to western Iowa during the day (figs. 6A and 6C). Warm, moist air from the Gulf of Mexico; warm, dry air from the southwestern United States; and cold, dry air from Canada was circulating into the low at low levels. The low sloped westward with height (figs. 6B and 6D) and a closed low at 500 mb moved from eastern Colorado to central Nebraska during the 12-hour period.

At 0600 CST a well-defined axis of moisture convergence (fig. 7A) extended around the low from central Texas to western South Dakota. The moisture requirements (fig. 7B) were not large over this area and had the same general orientation as the moisture convergence field. The presence of the warm, dry air in the southwestern sector of the low was reflected in the high values of lifted height (fig. 7C) and in the fields of moisture divergence and moisture requirements.

The agreement between the percent coverage field (fig. 7D) and the radar echo patterns (figs. 7E to 7G) was good throughout the 6-hour period. The agreement along the northwest-southeast portion of the main precipitation area was best at 0845 CST, and agreement

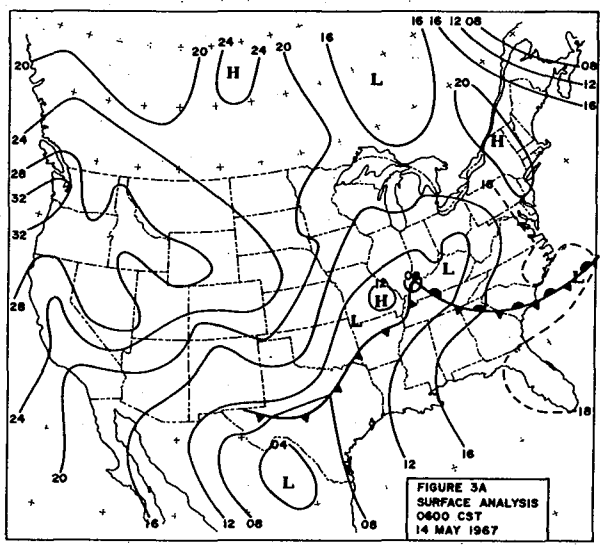

Figure 3A. Surface analysis for 0600 CST, 14 May 1967. Lines are isobars.

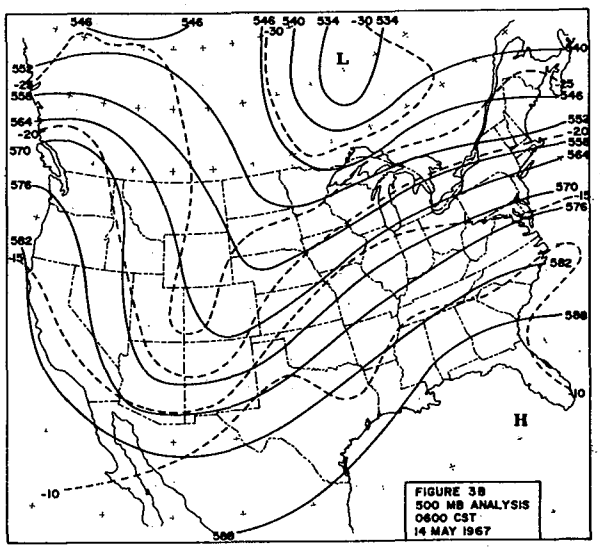

Figure 3B. 500-mb analysis for 0600 CST, 14 May 1967. Height contours are indicated by solid lines and are in tens of feet. Isotherms are indicated by dashed lines and are in °C.

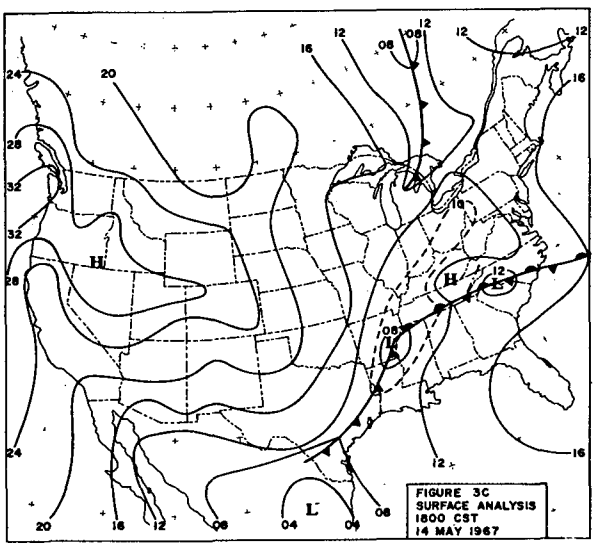

Figure 3C. Surface analysis for 1800 CST, 14 May 1967. Lines are isobars.

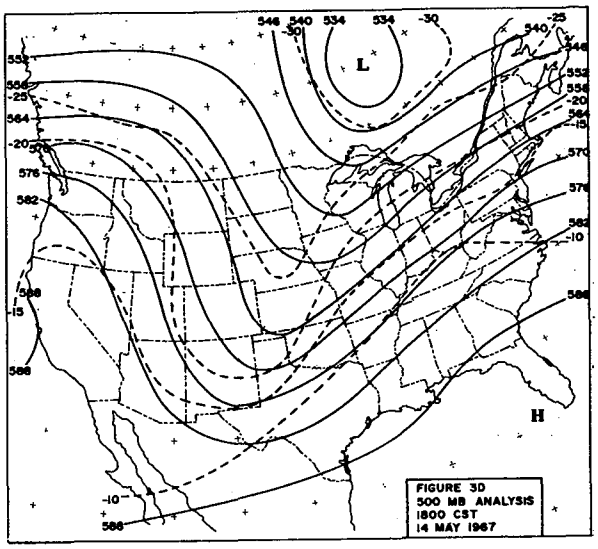

Figure 3D. 500-mb analysis for 1800 CST, 14 May 1967. Height contours are indicated by solid lines and are in tens of feet. Isotherms are indicated by dashed lines and are in °C.

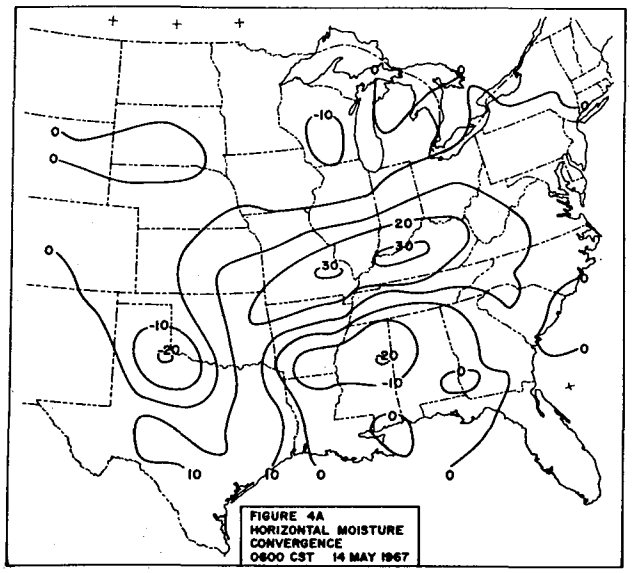

Figure 4A. Horizontal moisture divergence field (positive values indicate convergence) in the layer from the surface to 10,000 ft MSL for 0600 CST, 14 May 1967. Units are grams cm^{-2} $hour^{-1}$ in the column times 100.

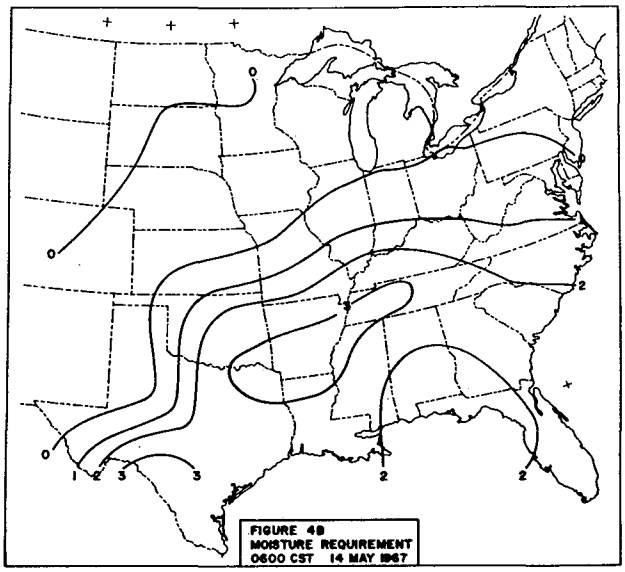

Figure 4B. Moisture requirement field in the layer from the lifting condensation level to 400 mb for 0600 CST, 14 May 1967. Units are grams cm^{-2} in the column.

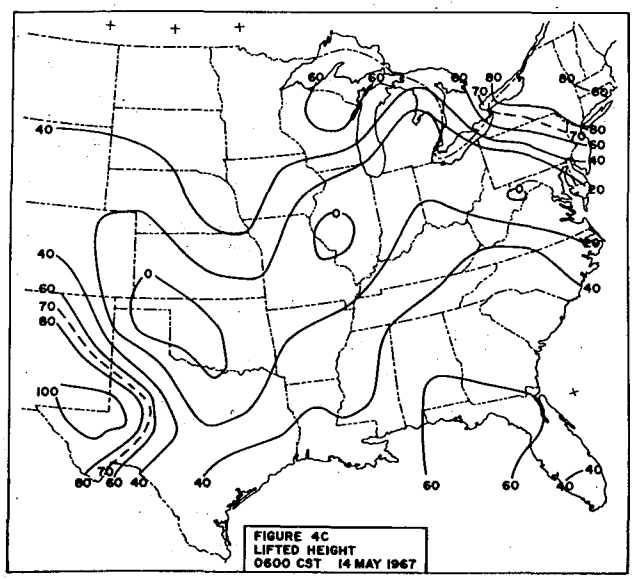

Figure 4C. Lifted height field for 0600 CST, 14 May 1967. Contours are in hundreds of feet. The 7000-ft contour is dashed.

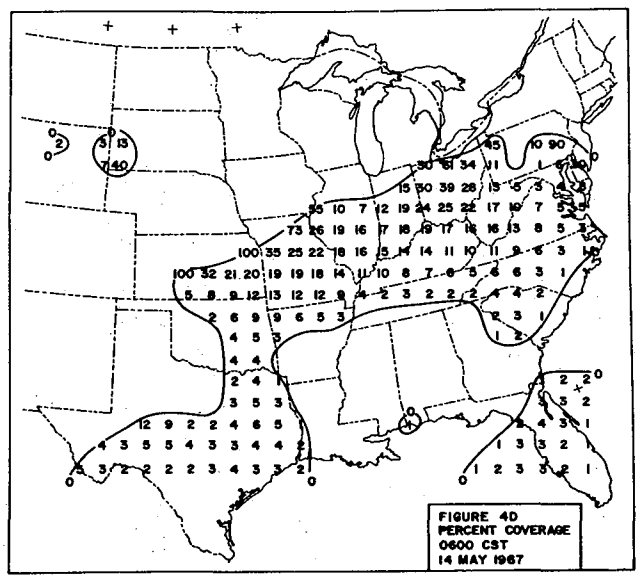

Figure 4D. Percent coverage field in percent for 0600 CST, 14 May 1967.

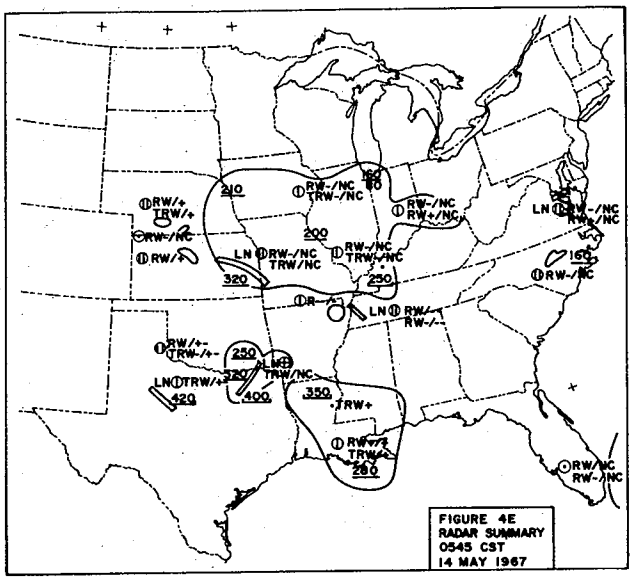

Figure 4E. Radar echo patterns at 0545 CST, 14 May 1967.

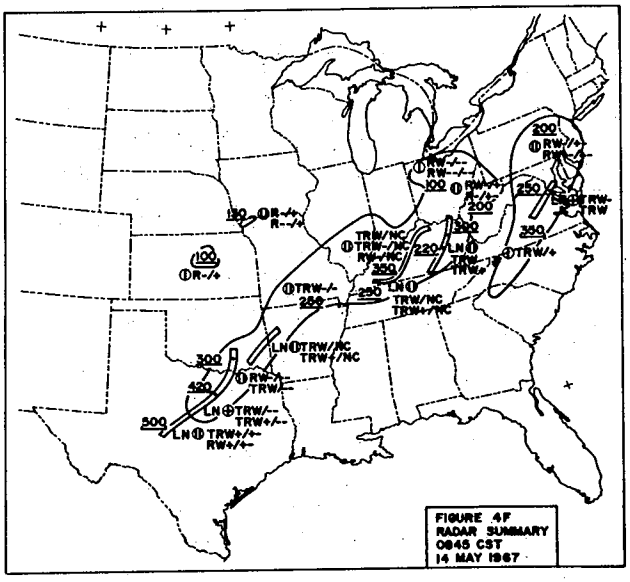

Figure 4F. Radar echo patterns at 0845 CST, 14 May 1967.

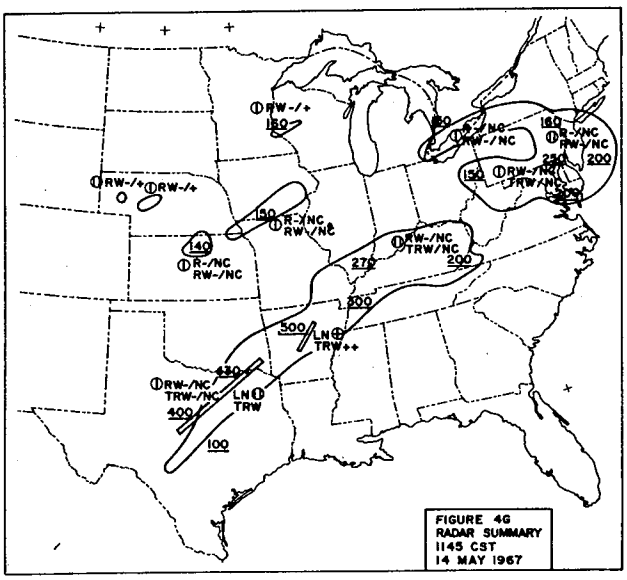

Figure 4G. Radar echo patterns at 1145 CST, 14 May 1967.

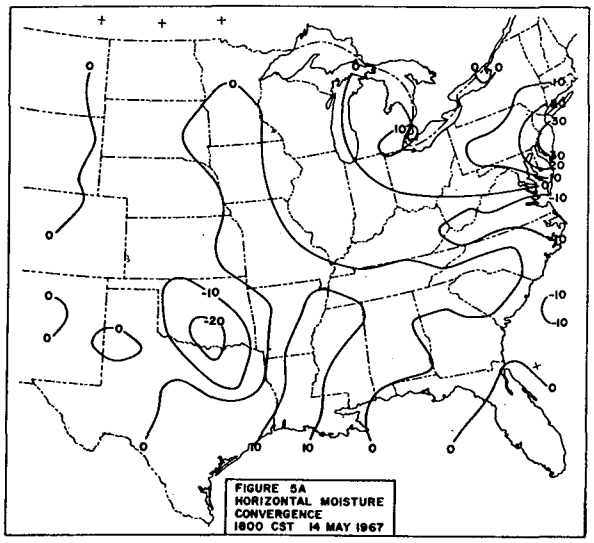

Figure 5A. Horizontal moisture divergence field (positive values indicate convergence) in the layer from the surface to 10,000 ft MSL for 1800 CST, 14 May 1967. Units are grams cm^{-2} $hour^{-1}$ in the column times 100.

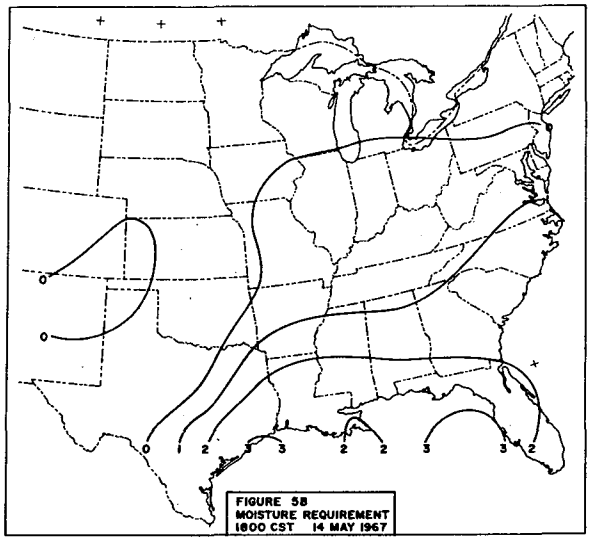

Figure 5B. Moisture requirement field in the layer from the lifting condensation level to 400 mb for 1800 CST, 14 May 1967. Units are grams cm^{-2} in the column.

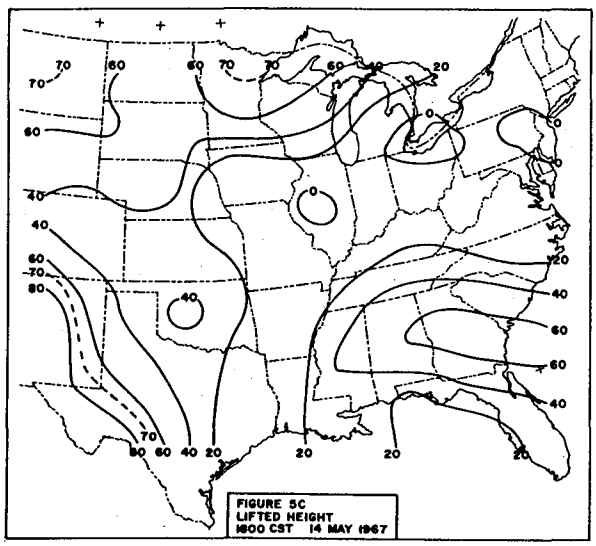

Figure 5C. Lifted height field for 1800 CST, 14 May 1967. Contours are in hundreds of feet. The 7000-ft contour is dashed.

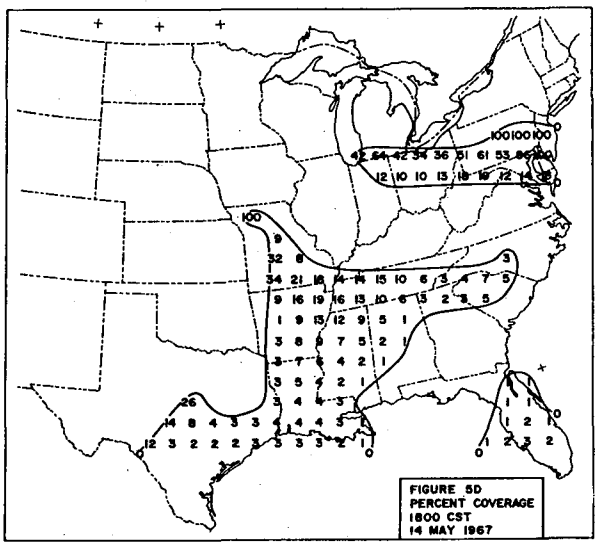

Figure 5D. Percent coverage field in percent for 1800 CST, 14 May 1967.

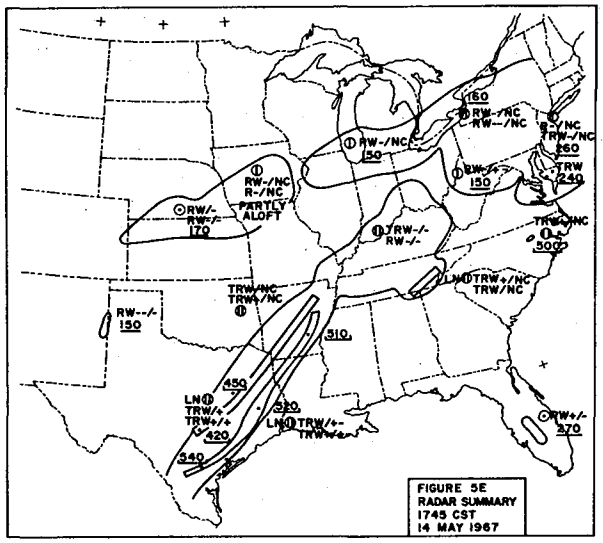

Figure 5E. Radar echo patterns at 1745 CST, 14 May 1967.

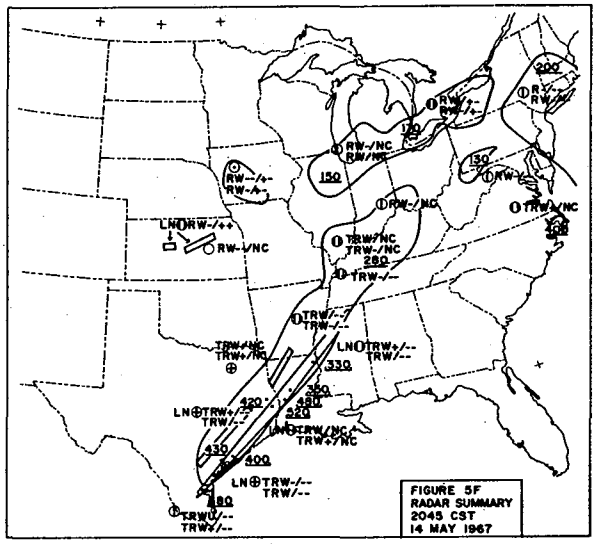

Figure 5F. Radar echo patterns at 2045 CST, 14 May 1967.

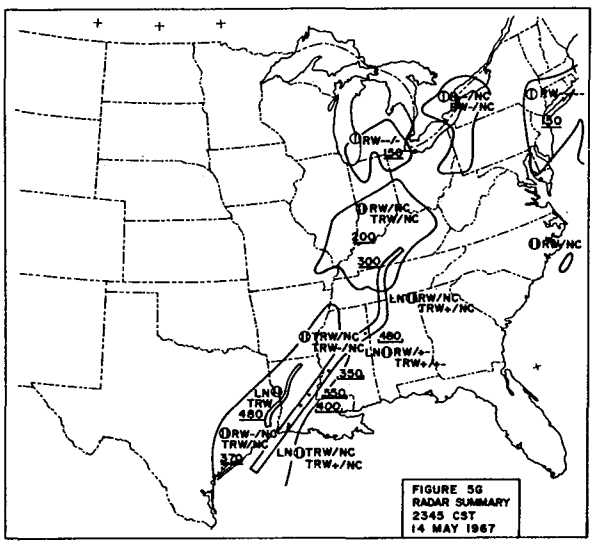

Figure 5G. Radar echo patterns at 2345 CST, 14 May 1967.

along the cold front improved as the convective activity moved into the area of highest percentages. There was considerable overprediction of the extent of coverage in the Mississippi-Alabama region. This was an area of moderately unstable air that apparently lacked a way to release the instability. The percentages are quite small in this area. The light rain in the North Carolina-South Carolina area was not predicted properly.

No severe weather was reported during the morning.

The axis of horizontal moisture convergence (fig. 8A) still extended around the surface low at 1800 CST but was no longer as well defined. The large percent coverage values around Lake Michigan (fig. 8D) were due primarily to the small moisture requirements (fig. 8B) that had changed from negative to positive during the day.

The radar echo patterns (figs. 8E to 8G) agreed well with the percent coverage field throughout the 6-hour period from 1800 to 2400 CST. This occurred because the percent coverage field was somewhat larger than the radar patterns and because the slowly moving radar areas maintained a stable configuration throughout the period.

The convection predicted at five grid points in the southwestern corner of the grid did not occur. These grid points had small moisture requirements, and three of the points had lifted height values greater than 6,000 ft (fig. 8C). Minor changes in the lifted height criteria at the latter grid points would have changed the percentages to zero. The other two points were, perhaps, areas of marginal convection.

Severe weather outbreaks occurred in a narrow zone along the Mississippi River from 33° N to 38° N between 1800 and 2200 CST. All occurrences were within the nonzero area.

7.3 Case 3 - 15 May 1968

A surface low in eastern Nebraska at 0600 CST (fig. 9A) deepened rapidly during the day and moved to southeastern Minnesota by evening (fig. 9C). A trough at 500 mb covered the western third of the country during the period (figs. 9B and 9D) with a short wave trough moving from Colorado to Kansas during the day.

Moisture convergence was occurring in most of the warm sector at 0600 CST (fig. 10A). Axes of moisture convergence, maximum moisture requirement (fig. 10B), and minimum lifted height (fig. 10C) extended northeastward from Texas. Large gradients of moisture requirements and lifted height occurred across the cold front.

Weak to moderate convective activity was occurring in the warm sector from Missouri to Ohio at 0545 CST (fig. 10E). By 0845 CST (fig. 10F) strong convection that became a squall line (fig. 10G,

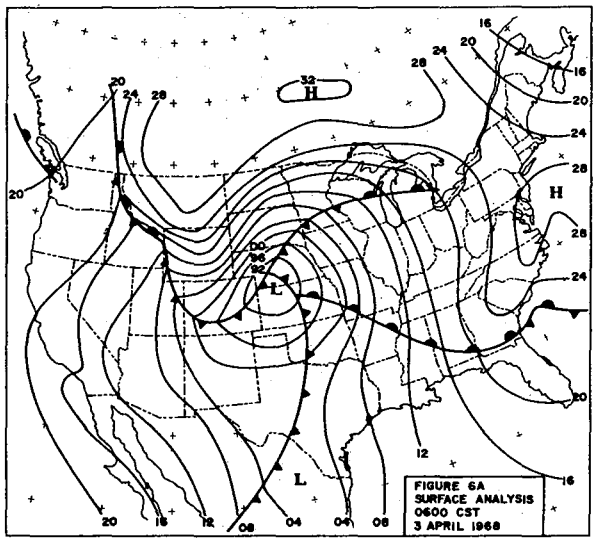

Figure 6A. Surface analysis for 0600 CST, 3 April 1968. Lines are isobars.

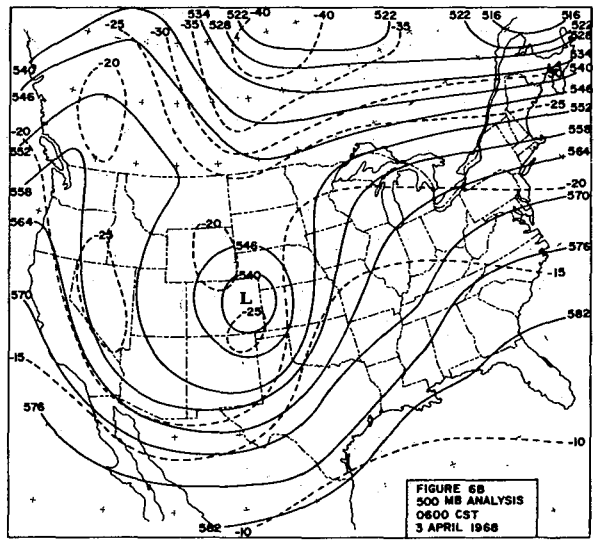

Figure 6B. 500-mb analysis for 0600 CST, 3 April 1968. Height contours are indicated by solid lines and are in tens of feet. Isotherms are indicated by dashed lines and are in °C.

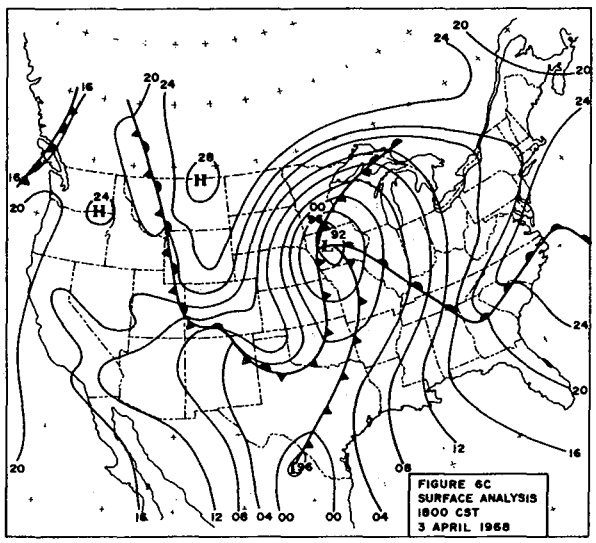

Figure 6C. Surface analysis for 1800 CST, 3 April 1968. Lines are isobars.

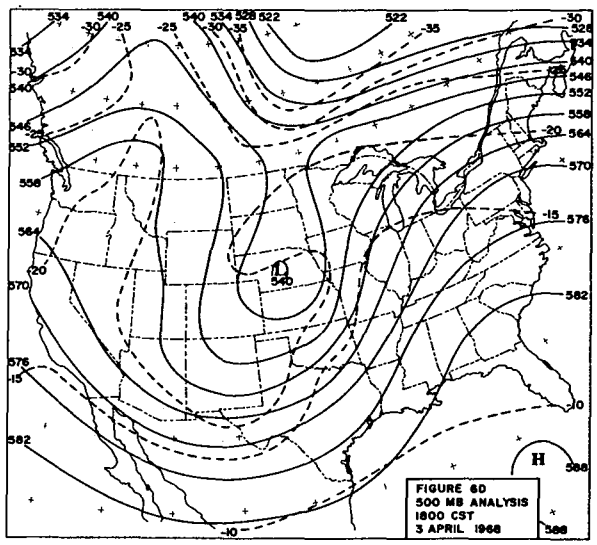

Figure 6D. 500-mb analysis for 1800 CST, 3 April 1968. Height contours are indicated by solid lines and are in tens of feet. Isotherms are indicated by dashed lines and are in °C.

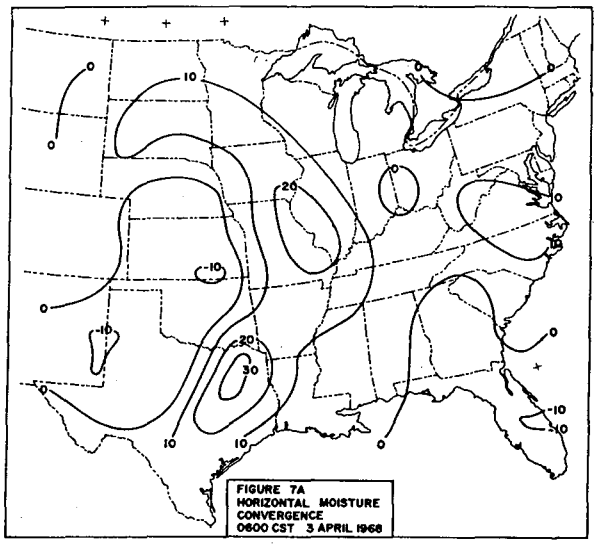

Figure 7A. Horizontal moisture divergence field (positive values indicate convergence) in the layer from the surface to 10,000 ft MSL for 0600 CST, 3 April 1968. Units are grams cm^{-2} $hour^{-1}$ in the column times 100.

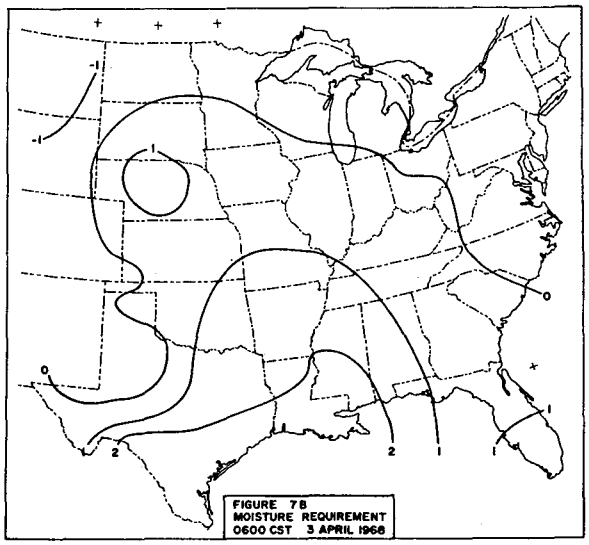

Figure 7B. Moisture requirement field in the layer from the lifting condensation level to 400 mb for 0600 CST, 3 April 1968. Units are grams cm^{-2} in the column.

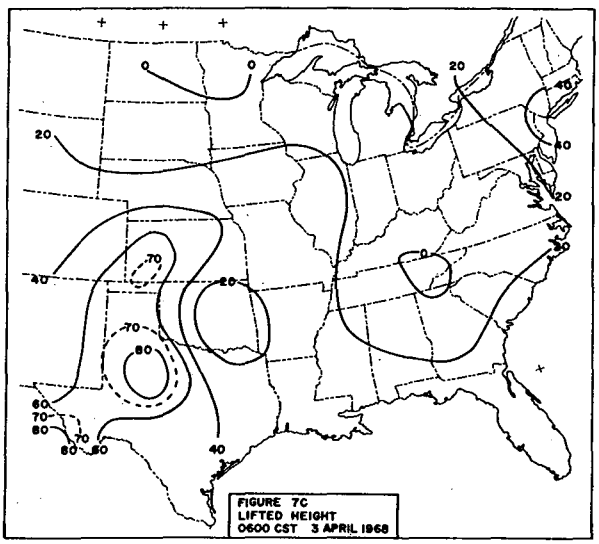

Figure 7C. Lifted height field for 0600 CST, 3 April 1968. Contours are in hundreds of feet. The 7000-ft contour is dashed.

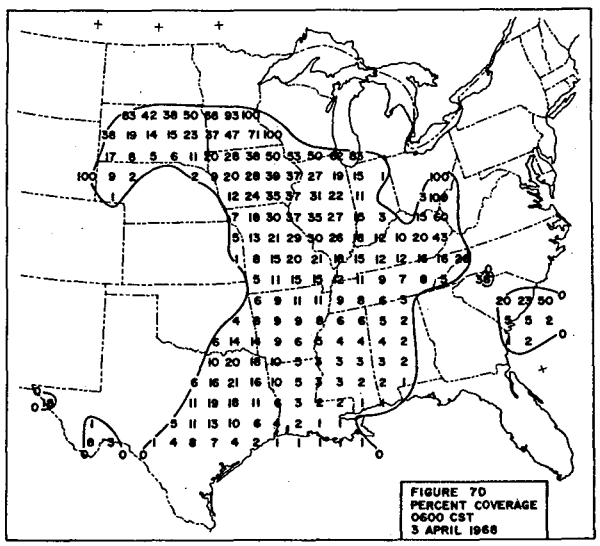

Figure 7D. Percent coverage field in percent for 0600 CST, 3 April 1968.

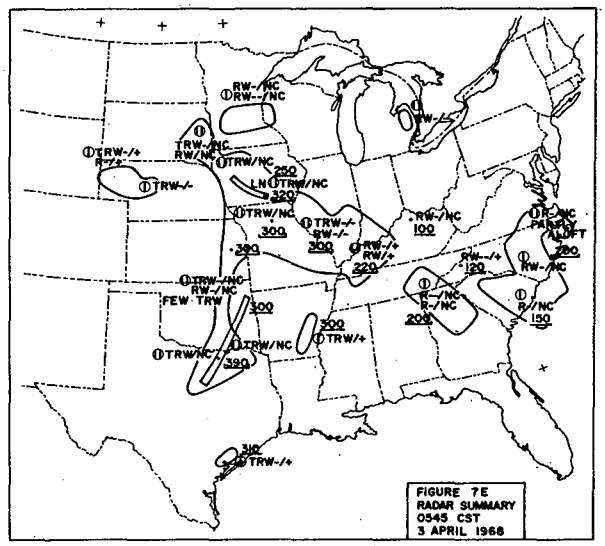

Figure 7E. Radar echo patterns at 0545 CST, 3 April 1968.

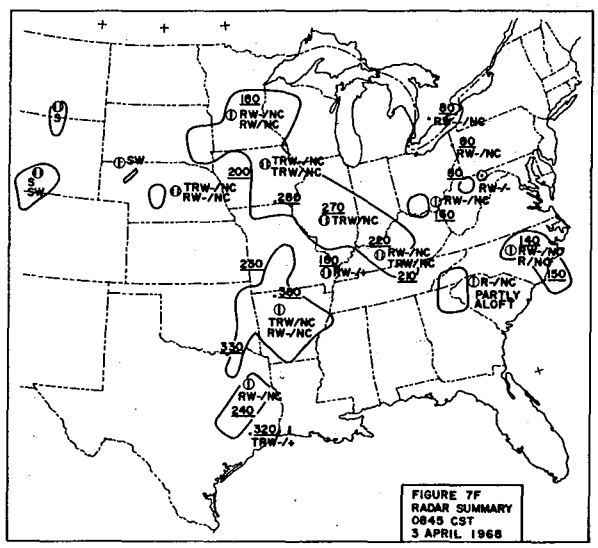

Figure 7F. Radar echo patterns at 0845 CST, 3 April 1968.

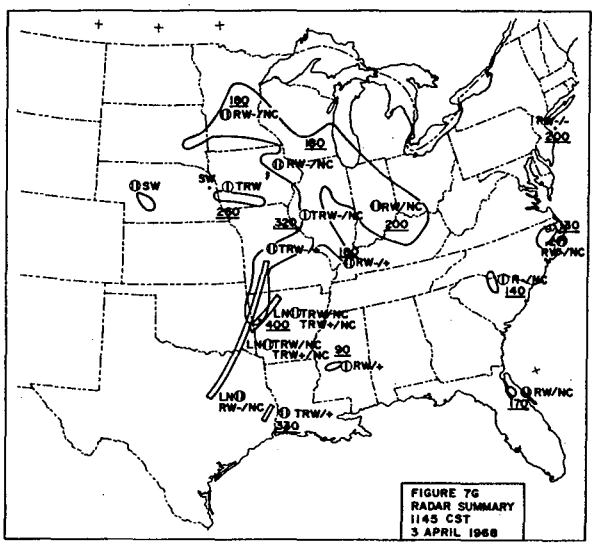

Figure 7G. Radar echo patterns at 1145 CST, 3 April 1968.

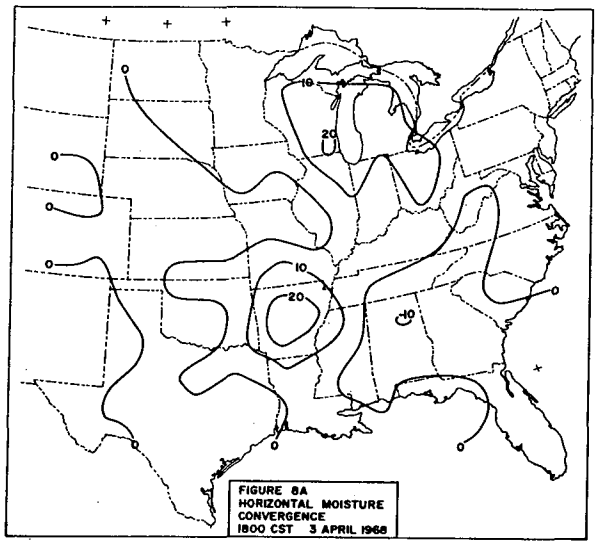

Figure 8A. Horizontal moisture divergence field (positive values indicate convergence) in the layer from the surface to 10,000 ft MSL for 1800 CST, 3 April 1968. Units are grams cm^{-2} $hour^{-1}$ in the column times 100.

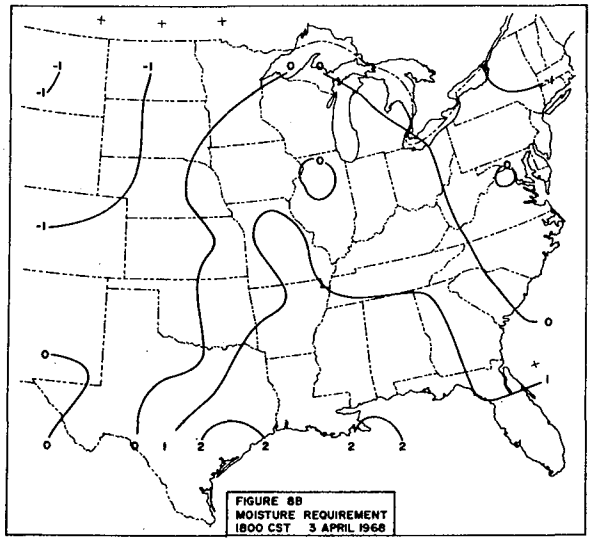

Figure 8B. Moisture requirement field in the layer from the lifting condensation level to 400 mb for 1800 CST, 3 April 1968. Units are grams cm^{-2} in the column.

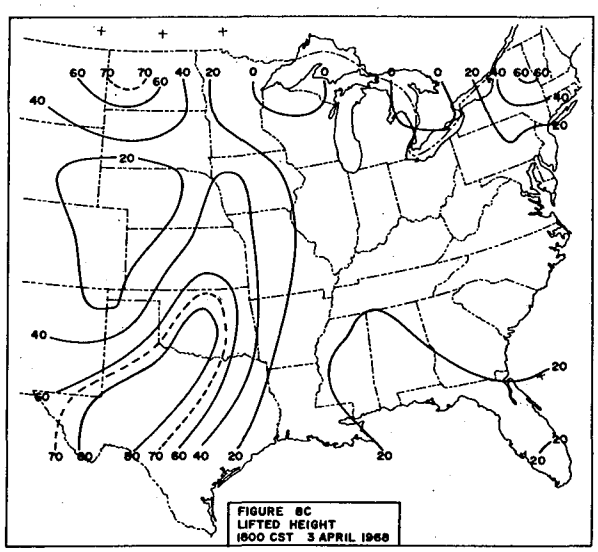

Figure 8C. Lifted height field for 1800 CST, 3 April 1968. Contours are in hundreds of feet. The 7000-ft contour is dashed.

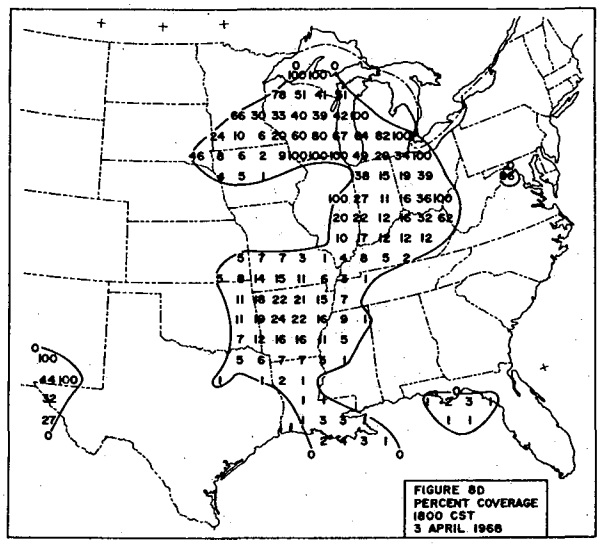

Figure 8D. Percent coverage field in percent for 1800 CST, 3 April 1968.

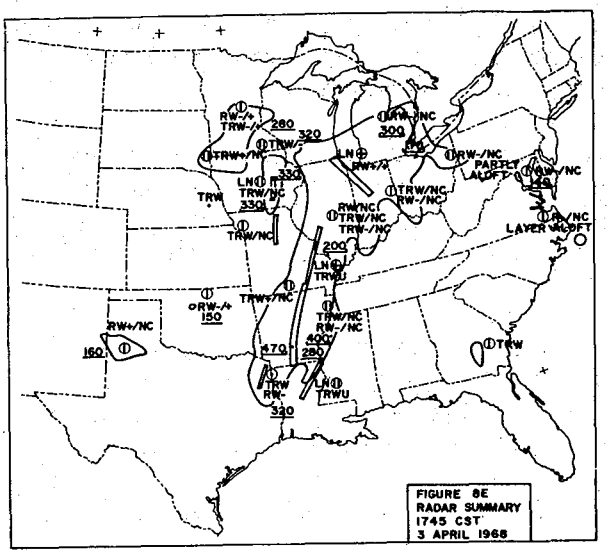

Figure 8E. Radar echo patterns at 1745 CST, 3 April 1968.

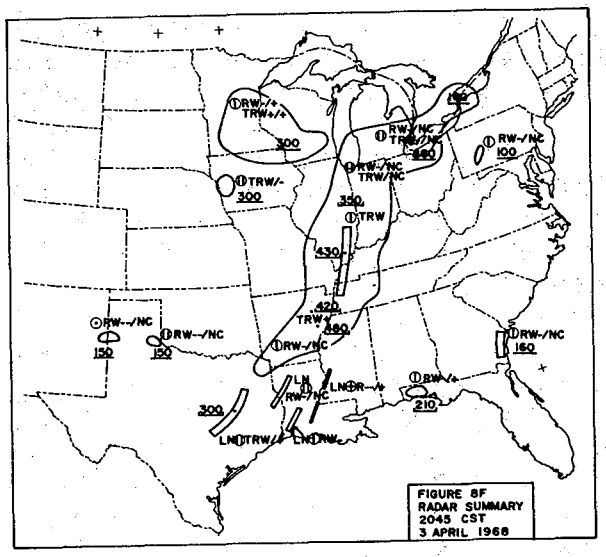

Figure 8F. Radar echo patterns at 2045 CST, 3 April 1968.

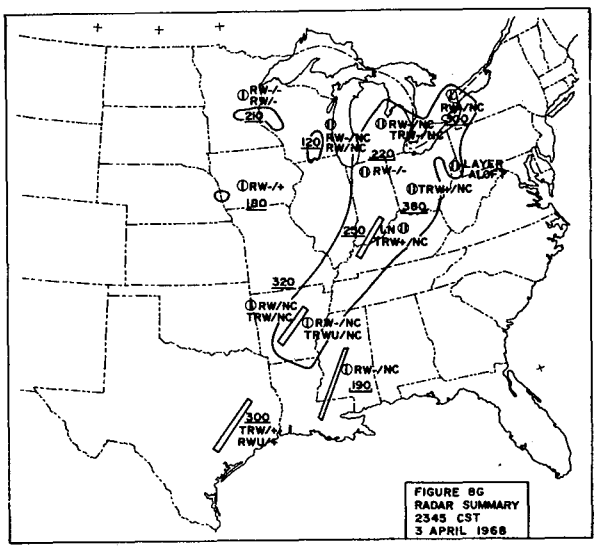

Figure 8G. Radar echo patterns at 2345 CST, 3 April 1968.

figs. 11E to 11G) had begun developing in Illinois, Iowa, and Oklahoma. However, the agreement between radar echo patterns and the percent coverage field (fig. 10D) is poor throughout the period.

The small percentages in the warm sector were a consequence of high moisture requirements and low moisture convergence. The zero percentage at the grid point in southeastern Missouri resulted from the procedure in the computer program of truncating to the whole percent.

The strong divergence-convergence couplet in the southeastern United States was unusual and was at first thought to be caused by bad data, but station data and objective analyses of the two components of horizontal moisture convergence appeared reasonable. The pattern was considered valid since a similar pattern was found at 1800 CST and since cumulus convection did occur at 0600 CST. A maximum of 10 to 12 percent coverage was found there at 0600 CST.

Wind and hail damage were observed in eastern Iowa and central Illinois during the morning. The reports in Iowa were in a region where the ratio was less than one percent and had been truncated to zero; the Illinois reports were in a region where the percentage was one.

By 1800 CST strong horizontal moisture convergence had developed over Illinois (fig. 11A); this was accompanied by a reduction in the moisture requirement (fig. 11B). Thus, the percent coverage (fig. 11D) was large in this region. An axis of minimum lifted height (fig. 11C), which had extended northward during the day, corresponded well with the north-south squall line at 1800 CST (fig. 11E).

The radar echo patterns (fig. 11E-G) moved from the western to the eastern portion of the nonzero area during the 6-hour period from 1800 to 2400 CST. The southern end of the convection extended southward into the divergence region which probably moved southeastward during the evening.

The divergence-convergence couplet and the accompanying convection in the southeastern United States moved southward during the day.

Severe weather occurred over a large portion of the warm sector during the evening. All reports of severe weather were within the nonzero area except three along the southern part of the squall line.

8. CONCLUSIONS

The technique works best in strong, well-defined synoptic situations. Generally, the correlation between the patterns of predicted cloud formation and the radar echo patterns is good at rawinsonde observation time, a little better three hours later, and decreases

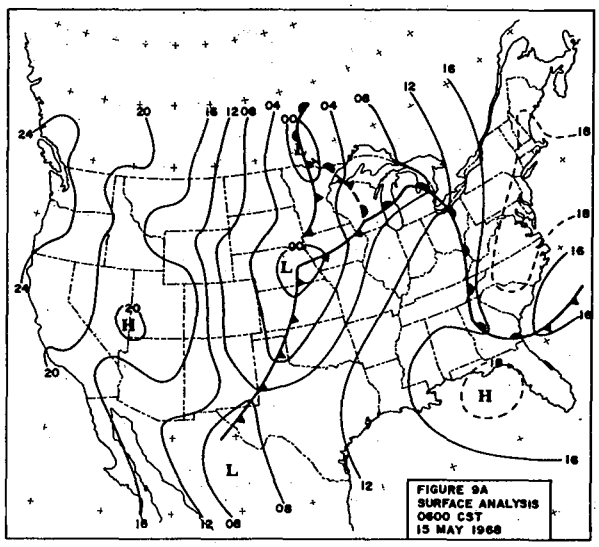

Figure 9A. Surface analysis for 0600 CST, 15 May 1968. Lines are isobars.

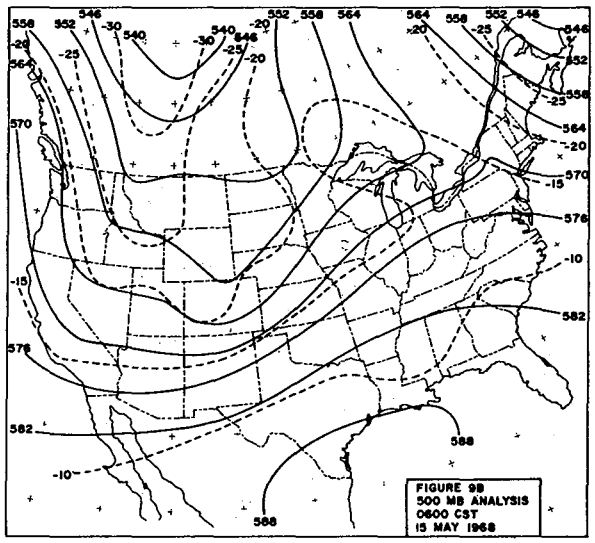

Figure 9B. 500-mb analysis for 0600 CST, 15 May 1968. Height contours are indicated by solid lines and are in tens of feet. Isotherms are indicated by dashed lines and are in °C.

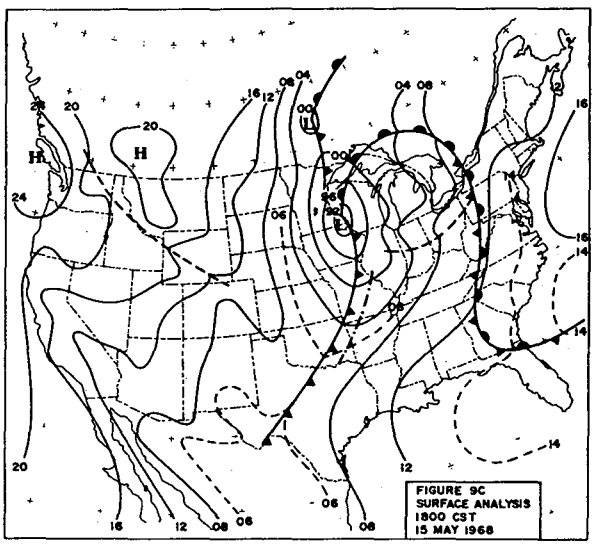

Figure 9C. Surface analysis for 1800 CST, 15 May 1968. Lines are isobars.

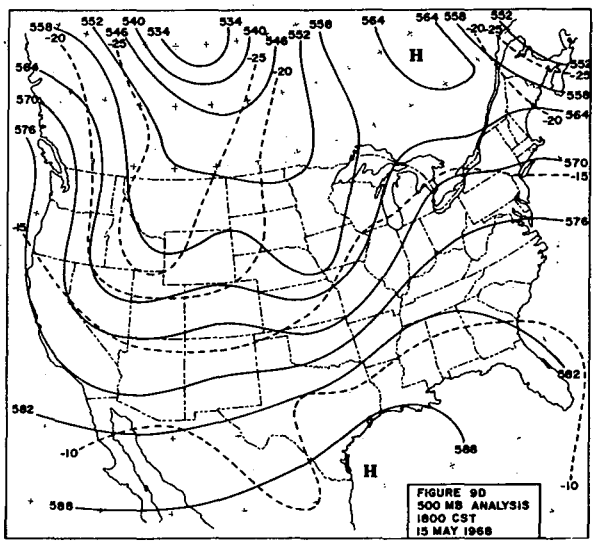

Figure 9D. 500-mb analysis for 1800 CST, 15 May 1968. Height contours are indicated by solid lines and are in tens of feet. Isotherms are indicated by dashed lines and are in °C.

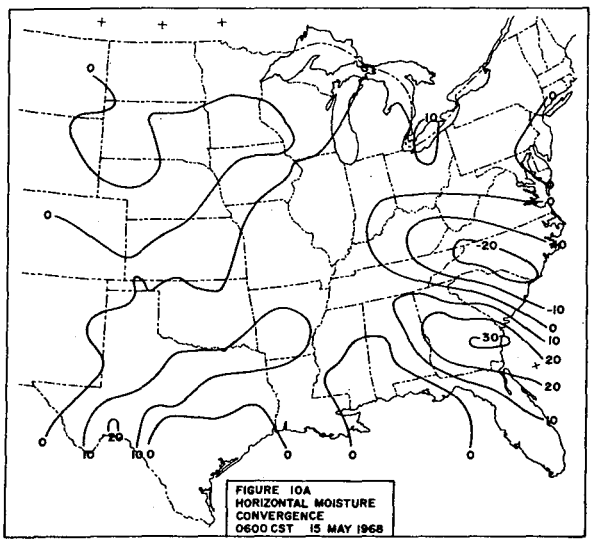

Figure 10A. Horizontal moisture divergence field (positive values indicate convergence) in the layer from the surface to 10,000 ft MSL for 0600 CST, 15 May 1968. Units are grams cm^{-2} $hour^{-1}$ in the column times 100.

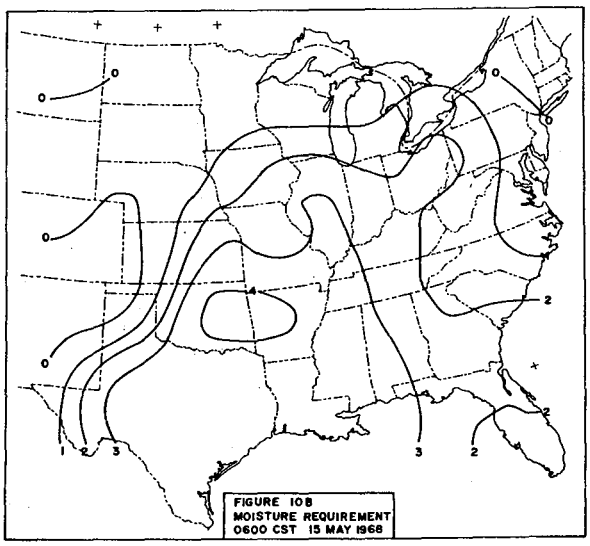

Figure 10B. Moisture requirement field in the layer from the lifting condensation level to 400 mb for 0600 CST, 15 May 1968. Units are grams cm^{-2} in the column.

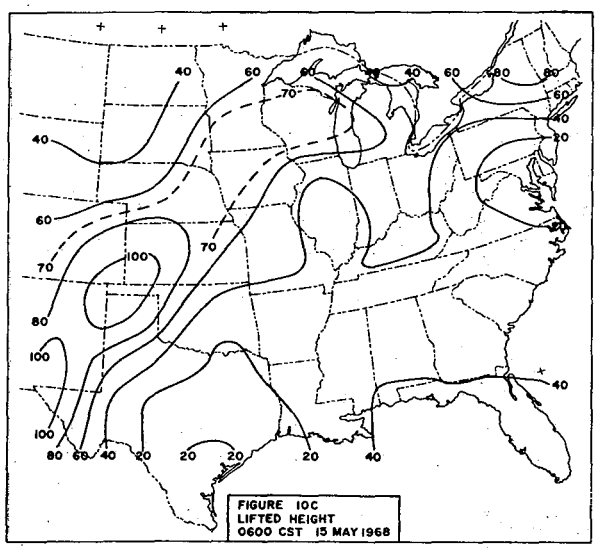

Figure 10C. Lifted height field for 0600 CST, 15 May 1968. Contours are in hundreds of feet. The 7000-ft contour is dashed.

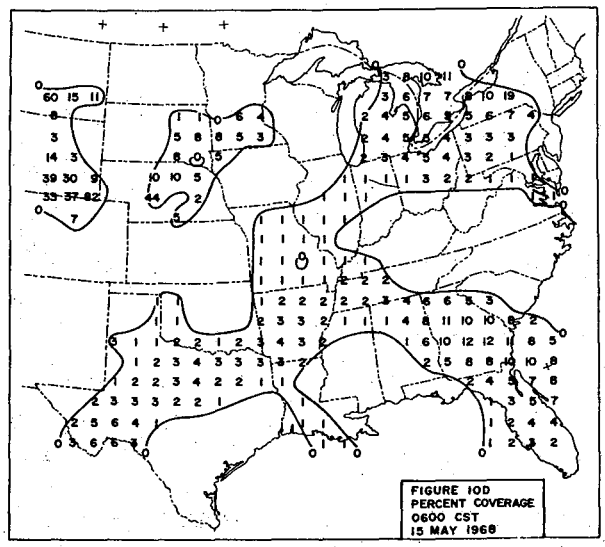

Figure 10D. Percent coverage field in percent for 0600 CST, 15 May 1968.

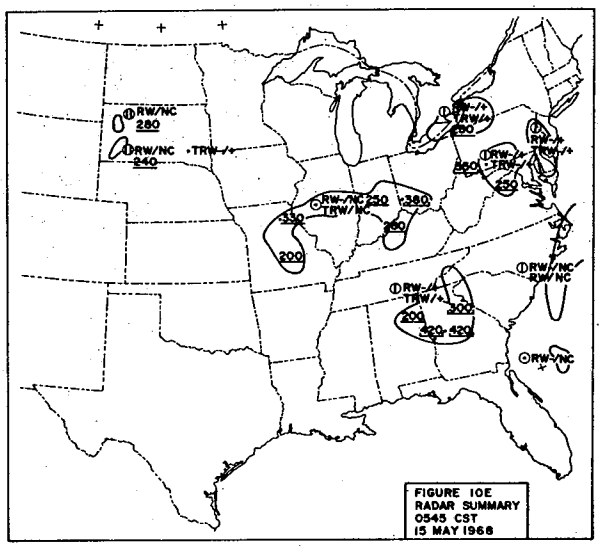

Figure 10E. Radar echo patterns at 0545 CST, 15 May 1968.

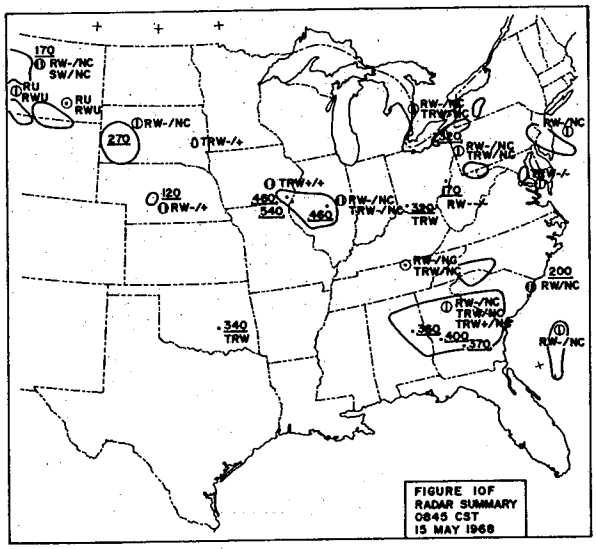

Figure 10F. Radar echo patterns at 0845 CST, 15 May 1968.

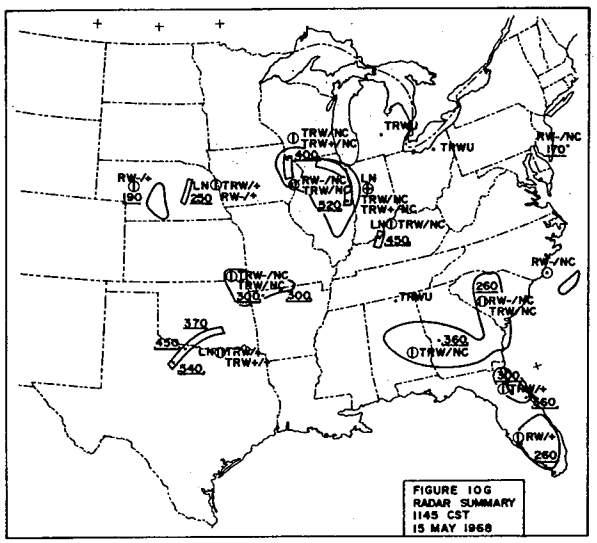

Figure 10G. Radar echo patterns at 1145 CST, 15 May 1968.

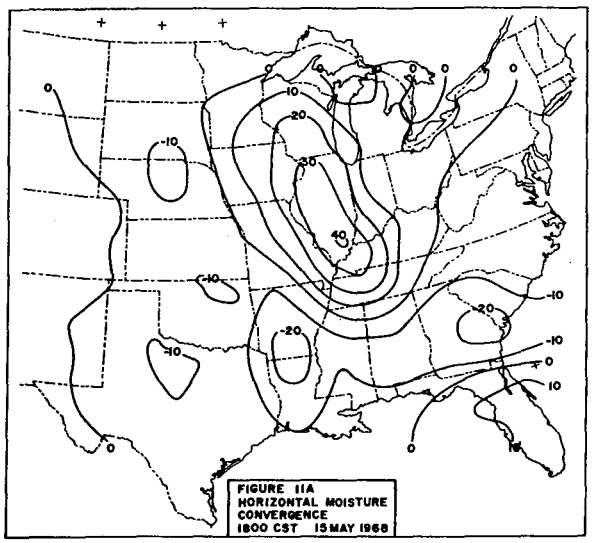

Figure 11A. Horizontal moisture divergence field (positive values indicate convergence) in the layer from the surface to 10,000 ft MSL for 1800 CST, 15 May 1968. Units are grams cm^{-2} $hour^{-1}$ in the column times 100.

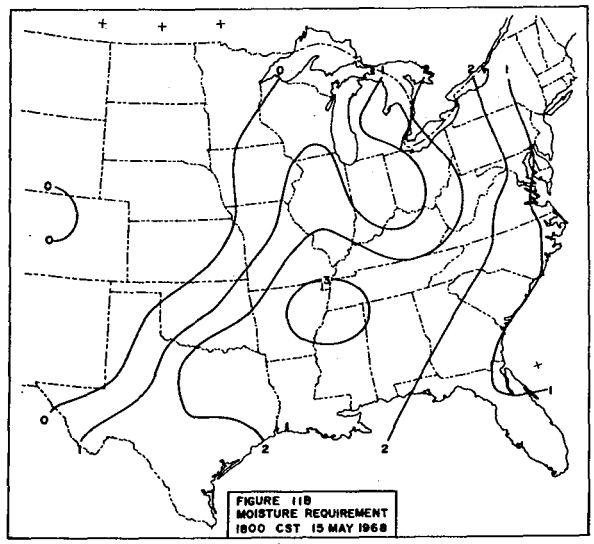

Figure 11B. Moisture requirement field in the layer from the lifting condensation level to 400 mb for 1800 CST, 15 May 1968. Units are grams cm^{-2} in the column.

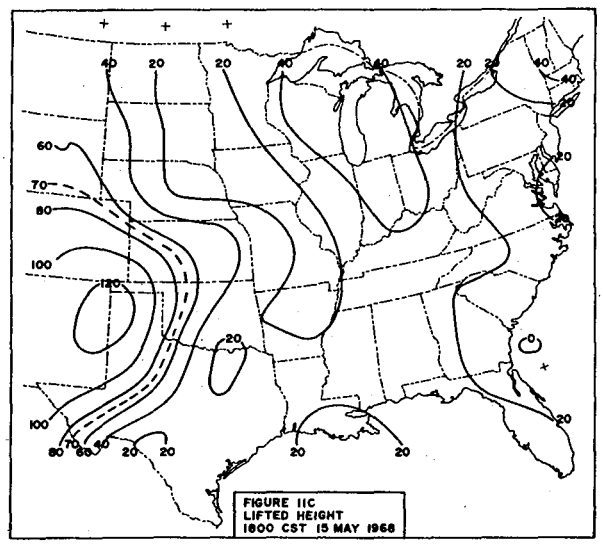

Figure 11C. Lifted height field for 1800 CST, 15 May 1968. Contours are in hundreds of feet. The 7000-ft contour is dashed.

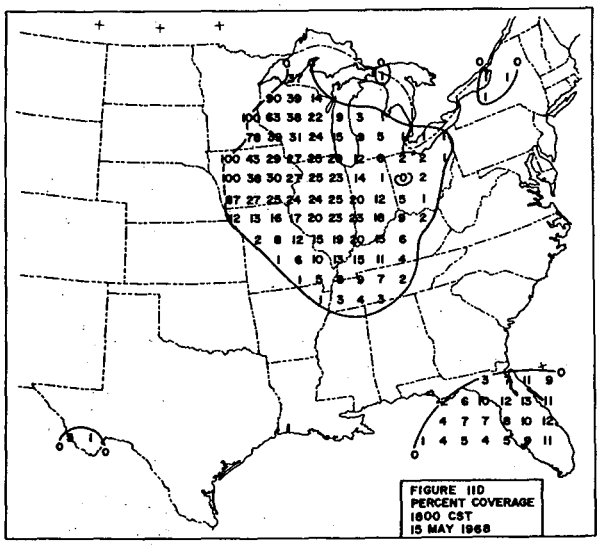

Figure 11D. Percent coverage field in percent for 1800 CST, 15 May 1968.

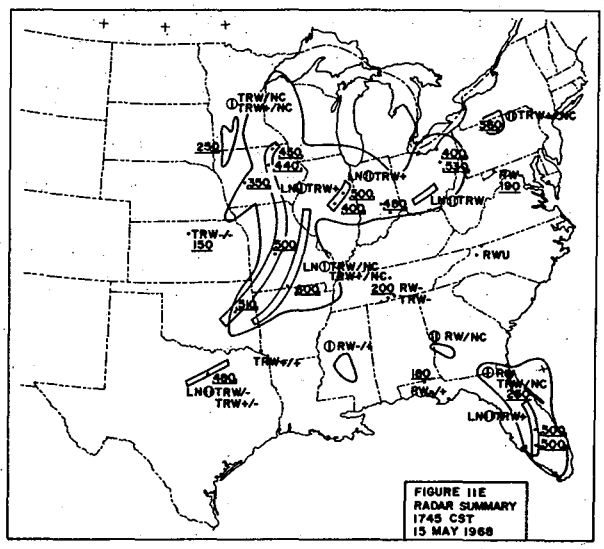

Figure 11E. Radar echo patterns at 1745 CST, 15 May 1968.

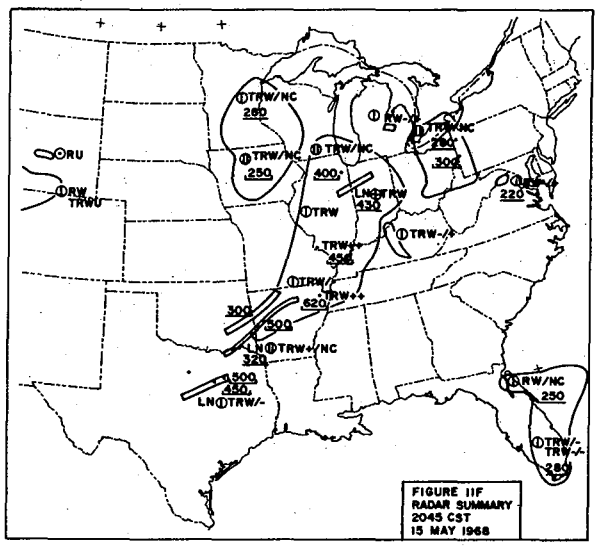

Figure 11F. Radar echo patterns at 2045 CST, 15 May 1968.

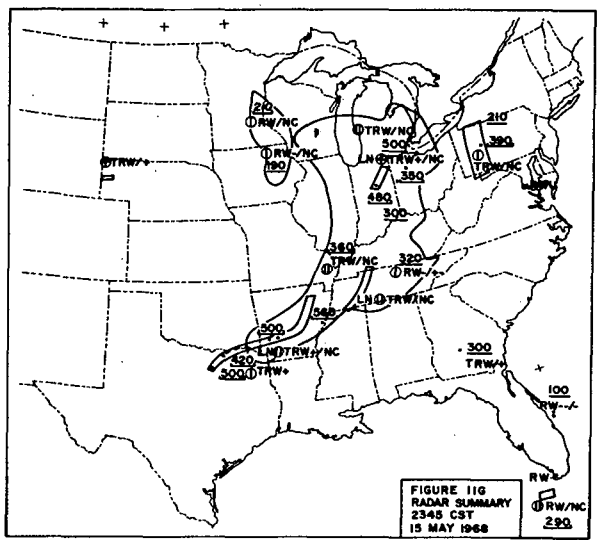

Figure 11G. Radar echo patterns at 2345 CST, 15 May 1968.

at greater time intervals between rawinsonde and radar observation times. Thus, the model is predictive on a short time scale rather than purely descriptive.

The orientation of the areas of nonzero percentages and, in particular, the relative maxima within nonzero areas agrees well with the orientation of convective cloud patterns. The model generally predicts zero percentage in areas of stratiform rain, a type of precipitation not adequately described by the model. Convection is often predicted over most of the warm sector of an extra-tropical cyclone. However, the percentages are usually less than five percent in portions of the warm sector that do not have radar echoes. Minima in the lifted height field are usually associated with considerable low-level moisture, especially in the warm sector of cyclones.

The examination of the 30 sets of data suggests that this parameterization technique can be of use as a kinematic short-range forecasting aid and may be applicable to numerical models designed for prediction of cumulus convection.

9. ACKNOWLEDGMENTS

Dr. Rex L. Inman suggested this study and provided guidance throughout the investigation.

The author would like to thank the staff of the National Severe Storms Forecast Center, Kansas City, Missouri, for providing computer time and programming assistance.

The author is indebted to Drs. Edwin Kessler, Gilbert D. Kinzer, and Ralph E. Pendleton for their critical reading of the manuscript.

10. REFERENCES

Charney, J. G., and A. Eliassen (1964), On the growth of the hurricane depression, J. Atmospheric Sci., 21, 68-75.

Cressman, G. P. (1959), An operational objective analysis system, Monthly Weather Rev., 87, 367-374.

Endlich, R. M., and R. L. Mancuso (1968), Objective analysis of environmental conditions associated with severe thunderstorms and tornadoes, Monthly Weather Rev., 96, 342-350.

Galway, J. G. (1956), The lifted index as a predictor of latent instability, Bull. Am. Meteorol. Soc., 37, 528-529.

Inman, R. L. (1968), Objective detection and correction of errors in radiosonde data, Tech. Memo ERLTM-NSSL 40, 48 pp.

Inman, R. L. (1969), Computation of temperature at the lifted condensation level, J. Appl. Meteorol., 8, 155-158.

Inman, R. L. (1970), Operational objective analysis schemes used at the National Severe Storms Forecast Center, Tech. Circular 10, NSSL.

Krishnamurti, T. N. (1968), A calculation of percentage area covered by convective clouds from moisture convergence, J. Appl. Meteorol., 7, 184-195.

Kuo, H. L. (1965), On formation and intensification of tropical cyclones through latent heat released by cumulus convection, J. Atmospheric Sci., 22, 40-63.

Ooyama, K. (1963), A dynamic model for the study of tropical cyclone development, Department of Meteorology and Oceanography, New York University, 26 pp.

Pearson, A. D. (1969), The tornado season of 1968, Weatherwise, 22, 21-25.

Phillips, N. A. (1957), A map projection system suitable for large-scale numerical weather prediction, Seventy-fifth Anniversary Volume of the Journal of the Meteorological Society of Japan, 262-267.

Prosser, N. E., and D. S. Foster (1966), Upper air sounding analysis by use of an electronic computer, J. Appl. Meteorol., 5, 296-300.

Sasaki, Y. (1964), Preliminary results of numerical forecasting of small-scale convective activities, Final Report for NSF G-19688, Atmospheric Research Lab, University of Oklahoma Research Institute, Norman, Oklahoma, 12 pp.

Showalter, A. K. (1953), A stability index for thunderstorm forecasting, Bull. Am. Meteorol. Soc., 34, 250-252.

NATIONAL SEVERE STORMS LABORATORY

The NSSL Technical Memoranda, beginning with No. 28, continue the sequence established by the U. S. Weather Bureau National Severe Storms Project, Kansas City, Missouri. Numbers 1-22 were designated NSSP Reports. Numbers 23-27 were NSSL Reports, and 24-27 appeared as subseries of Weather Bureau Technical Notes. These reports are available from the Clearinghouse for Federal Scientific and Technical Information, 5285 Port Royal Road, Springfield, Virginia 22151, for $3.00, and a microfiche version for $0.65. CFTSI numbers are given below in parentheses.

No. 1 National Severe Storms Project Objectives and Basic Design. Staff, NSSP. March 1961. (PB-168207)

No. 2 The Development of Aircraft Investigations of Squall Lines from 1956-1960. B. B. Goddard. (PB-168208)

No. 3 Instability Lines and Their Environments as Shown by Aircraft Soundings and Quasi-Horizontal Traverses. D. T. Williams. February 1962. (PB-168209)

No. 4 On the Mechanics of the Tornado. J. R. Fulks. February 1962. (PB-168210)

No. 5 A Summary of Field Operations and Data Collection by the National Severe Storms Project in Spring 1961. J. T. Lee. March 1962. (PB-165095)

No. 6 Index to the NSSP Surface Network. T. Fujita. April 1962. (PB-168212)

No. 7 The Vertical Structure of Three Dry Lines as Revealed by Aircraft Traverses. E. L. McGuire. April 1962. (PB-168213)

No. 8 Radar Observations of a Tornado Thunderstorm in Vertical Section. Ralph J. Donaldson, Jr. April 1962. (PB-174859)

No. 9 Dynamics of Severe Convective Storms. Chester W. Newton. July 1962. (PB-163319)

No. 10 Some Measured Characteristics of Severe Storms Turbulence. Roy Steiner and Richard H. Rhyne. July 1962. (N62-16401)

No. 11 A Study of the Kinematic Properties of Certain Small-Scale Systems. D. T. Williams. October 1962. (PB-168216)

No. 12 Analysis of the Severe Weather Factor in Automatic Control of Air Route Traffic. W. Boynton Beckwith. December 1962. (PB-168217)

No. 13 500-Kc./Sec. Sferics Studies in Severe Storms. Douglas A. Kohl and John E. Miller. April 1963. (PB-168218)

No. 14 Field Operations of the National Severe Storms Project in Spring 1962. L. D. Sanders. May 1963. (PB-168219)

No. 15 Penetrations of Thunderstorms by an Aircraft Flying at Supersonic Speeds. G. P. Roys. Radar Photographs and Gust Loads in Three Storms of 1961 Rough Rider. Paul W. J. Schumacher. May 1963. (PB-168220)

No. 16 Analysis of Selected Aircraft Data from NSSP Operations, 1962. T. Fujita. May 1963. (PB-168221)

No. 17 Analysis of Methods for Small-Scale Surface Network Data. D. T. Williams. August 1963. (PB-168222)

No. 18 The Thunderstorm Wake of May 4, 1961. D. T. Williams. August 1963. (PB-168223)

No. 19 Measurements by Aircraft of Condensed Water in Great Plains Thunderstorms. George P. Roys and Edwin Kessler. July 1966. (PB-173048)

No. 20 Field Operations of the National Severe Storms Project in Spring 1963. J. T. Lee, L. D. Sanders and D. T. Williams. January 1964. (PB-168224)

No. 21 On the Motion and Predictability of Convective Systems as Related to the Upper Winds in a Case of Small Turning of Wind with Height. James C. Fankhauser. January 1964. (PB-168225)

No. 22 Movement and Development Patterns of Convective Storms and Forecasting the Probability of Storm Passage at a Given Location. Chester W. Newton and James C. Fankhauser. January 1964. (PB-168226)

No. 23 Purposes and Programs of the National Severe Storms Laboratory, Norman, Oklahoma. Edwin Kessler. December 1964. (PB-166675)

No. 24 Papers on Weather Radar, Atmospheric Turbulence, Sferics, and Data Processing. August 1965. (AD-621586)

No. 25 A Comparison of Kinematically Computed Precipitation with Observed Convective Rainfall. James C. Fankhauser. September 1965. (PB-168445).

GPO 857-965

No. 26 Probing Air Motion by Doppler Analysis of Radar Clear Air Returns. Roger M. Lhermitte. May 1966. (PB-170636)

No. 27 Statistical Properties of Radar Echo Patterns and the Radar Echo Process. Larry Armijo. May 1966. The Role of the Kutta-Joukowski Force in Cloud Systems with Circulation. J. L. Goldman. May 1966. (PB-170756)

No. 28 Movement and Predictablity of Radar Echoes. James Warren Wilson. November 1966. (PB-173972)

No. 29 Notes on Thunderstorm Motions, Heights, and Circulations. T. W. Harrold, W. T. Roach, and Kenneth E. Wilk. November 1966. (AD-644899)

No. 30 Turbulence in Clear Air Near Thunderstorms. Anne Burns, Terence W. Harrold, Jack Burnham, and Clifford S. Spavins. December 1966. (PB-173992)

No. 31 Study of a Left-Moving Thunderstorm of 23 April 1964. George R. Hammond. April 1967. (PB-174681)

No. 32 Thunderstorm Circulations and Turbulence from Aircraft and Radar Data. James C. Fankhauser and J. T. Lee. April 1967. (PB-174860)

No. 33 On the Continuity of Water Substance. Edwin Kessler. April 1967. (PB-175840)

No. 34 Note on the Probing Balloon Motion by Doppler Radar. Roger M. Lhermitte. July 1967. (PB-175930)

No. 35 A Theory for the Determination of Wind and Precipitation Velocities with Doppler Radars. Larry Armijo. August 1967. (PB-176376)

No. 36 A Preliminary Evaluation of the F-100 Rough Rider Turbulence Measurement System. U. O. Lappe. October 1967. (PB-177037)

No. 37 Preliminary Quantitative Analysis of Airborne Weather Radar. Lester P. Merritt. December 1967. (PB-177188)

No. 38 On the Source of Thunderstorm Rotation. Stanley L. Barnes. March 1968. (PB-178990)

No. 39 Thunderstorm - Environment Interactions Revealed by Chaff Trajectories in the Mid-Troposphere. James C. Fankhauser. June 1968. (PB-179659)

No. 40 Objective Detection and Correction of Errors in Radiosonde Data. Rex L. Inman. June 1968. (PB-180284)

No. 41 Structure and Movement of the Severe Thunderstorms of 3 April 1964 as Revealed from Radar and Surface Mesonetwork Data Analysis. Jess Charba and Yoshikazu Sasaki. October 1968. (PB-183310)

No. 42 A Rainfall Rate Sensor. Brian E. Morgan. November 1968. (PB-183979)

No. 43 Detection and Presentation of Severe Thunderstorms by Airborne and Ground-Based Radars: A Comparative Study. Kenneth E. Wilk, John K. Carter, and J. T. Dooley. February 1969. (PB-183572)

No. 44 A Study of a Severe Local Storm of 16 April 1967. George Thomas Haglund. May 1969. (PB-184-970)